DISSIPATIVE HEAT TRANSFER ON HYDROMAGNETIC FLOW OF COPPER AND ALUMINA ETHYLENE-GLYCOL BASED NANOFLUID OVER A HEATED VERTICAL PLATE

BY

MWAIGHACHO ETHEL (B.Ed. (Science))

REG NO: I56/CE/34187/2017

MATHEMATICS DEPARTMENT

A RESEARCH PROJECT SUBMITTED IN PARTIAL FULFILLMENT OF THE REQUIREMENT FOR THE AWARD OF THE DEGREE OF MASTERS OF SCIENCE IN APPLIED MATHEMATICS IN THE SCHOOL OF PURE AND APPLIED SCIENCES OF KENYATTA UNIVERSITY

JUNE, 2021.

DECLARATION

I hereby declare that this project is my original work and has not been submitted to any university, in part or whole, for a degree award.

Signature……. Date……11/06/2021……

ETHEL MWAIGHACHO

B.Ed.Sci (Hons.)

This project has been submitted for examination to the school of pure and applied sciences with my approval as the university supervisor.

Signature…….. Date……

DR. WINIFRED NDUKU MUTUKU

Department of Mathematics and Actuarial Science

Kenyatta University

DEDICATION

I would like to dedicate this work to my son Adrian Ratumo and my brothers Christopher Kombo and Peter Mwangima. May you find the inner strength and ability to achieve all what you desire in life.

ACKNOWLEGEMENTS

First I would like to thank the Almighty God for enabling me reach this far, for his love, blessings and sufficient grace have made this to be achievable.

I wish to express my sincere gratitude to my supervisor, Dr. Winfred Mutuku who dedicated her time and support to ensure that this research work was a success. The discussions we had and the constant checking on my progress enabled me to finish this within the required time, am grateful for that.

To my friend Juma Mwamunga, you've been my support system throughout this study. Thank you for encouraging me and always reminding me that I could take this challenge. Your moral and financial support will never be forgotten for they enabled me to undertake this study successfully.

To my friends Abayomi Oke and my course mates Priscilla, Olum and Wekesa, you've always given me the challenge to work harder, your efforts can never go unnoticed.

Lastly, to my siblings Shirley, Kambe, Chris, Peter and Ringo, you ensured that my learning was so smooth by taking care of my duties when I was studying. I am so lucky to be a part of you.

PUBLISHED WORK

E. Mwaighacho,W.Mutuku,(2020). Dissipative Heat Transfer on Hydromagnetic Flow of Copper and Alumina Ethylene- Glycol Based Nanofluid over A Heated Vertical Plate. *IOSR Jounal of Mathematics,16(5);34-43,e-ISSN:2278-5728,p-ISSN:2319-765X*

ABSTRACT

In this study, the dissipative heat transfer of magnetohydrodynamic nanofluid with Ethylene-Glycol as the base fluid containing copper and Alumina as the nanoparticles is considered. The steady viscous flow of the electrically conducting liquid is considered to be along a heated vertical plate. The transformed boundary layer equations are non-dimensionalized using appropriate similarity variables and solved using the fourth-order Runge-Kutta method coupled with a shooting technique. The influence of pertinent parameters on velocity profile, temperature profile, skin friction and Nusselt number are investigated and the results analyzed graphically using MATLAB. The results obtained in velocity, temperature and concentration profiles were in good agreement with the actual flow dynamics. Al_2O_3-Ethylene glycol-based nanofluid had the highest skin friction while Cu-Ethylene glycol-based nanofluid had higher heat and mass transfer rates.

TABLE OF CONTENTS

LIST OF FIGURES

LIST OF TABLES

NOMENCLATURE

(u, v)	Velocity components in x and y direction
x, y	Spatial Coordinates
B_o	Constant applied magnetic field
c_p	Specific heat at constant pressure
Pr	Prandtl Number
Ec	Eckert Number
Gr	Grashof Number
Bi	Local Biot Number
Sc	Schmidt Number
M	Magnetic field parameter
D_B	Brownian diffusion coefficient
C	Concentration at any point in the flow field
C_w	Concentration at the wall
C_∞	Concentration at the free stream
T	Temperature of the fluid
T_w	Temperature at the wall
T_∞	Temperature of the fluid far from the plate
h_f	Heat transfer coefficient
k	Thermal conductivity
g	Acceleration due to gravity

Greek Letters

ψ	Stream function
θ	Dimensionless temperature
ϕ	Dimensionless concentration
η	Similarity variable
β	Thermal expansion coefficient
α	Thermal diffusivity
μ	Dynamic viscosity
υ	Kinematic viscosity
σ	Electrical conductivity
ρ	Density
φ	Nanoparticle concentration

Subscripts

bf	Base fluid
np	Nanoparticles
nf	Nanofluids

Abbreviations

MHD	Magnetohydrodynamic
PDEs	Partial Differential Equations
ODEs	Ordinary Differential Equations
RHS	Right Hand Side
LHS	Left Hand Side

CHAPTER ONE

INTRODUCTION

1.0. Overview

In this chapter, we have defined key terminologies used in this research. A review of the related literature to this work is given and the statement of the problem is also put forward. Objectives, significance, justification and applications of the study are outlined too.

1.1. Background Information

Heat transfer has extensive applications in the cooling and heating of fluids in industrial processes. The enhancement of these processes has been embraced since the commonly used base fluids such as water, ethylene glycol and engine oil have low thermal conductivities making them less efficient in heat transfer. To improve the heat transfer efficiency, small solid particles are added to the base fluids to form nanofluids. Nanofluids have better thermophysical properties since the solids particles added to them have a high thermal conductivity. This makes the novel fluid have wide applications in industrial processes. In this study, the dissipative heat transfer of magnetohydrodynamic nanofluids is considered. The flow of the nanofluid is past a heated vertical plate hence causing a boundary layer flow.

1.2. Hydromagnetic

Hydromagnetic (MHD) describes electrically conducting fluids in which a magnetic field is present. This was first discussed by Hannes Alfven in 1908-1995. These conducting fluids include liquid metals, plasmas (such as solar atmosphere) and strong electrolytes. The rationale behind MHD is that the interaction between the magnetic field and the conducting fluids induces an electric current of density $\boldsymbol{j}$ into the conducting fluid resulting in an induced magnetic field. The net magnetic field $\boldsymbol{B}$ interacts with the induced current $\boldsymbol{j}$ resulting in Lorentz force, $\boldsymbol{F} = \boldsymbol{j} \times \boldsymbol{B}$. The interaction of the moving conducting fluids with electric and

magnetic fields provides for a rich variety of phenomena associated with electro-fluid-mechanical energy conversion.

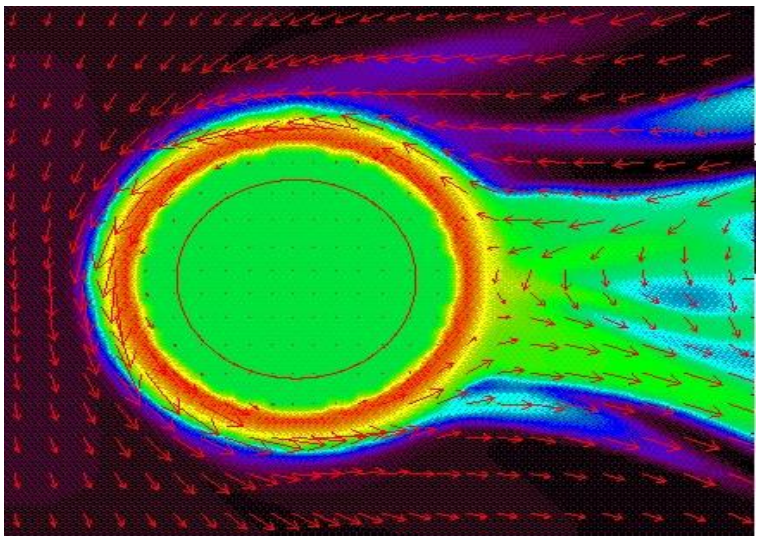

Figure.1.1: Magnetohydrodynamic flow (source:https://sites.google.com/site/iranmhd/what-is-mhd)

The effects of such interactions can be observed in liquids, gases, two-phase mixtures or plasmas. Numerous applications of MHD exist such as heating and flow control in metals processing, magnetic confinement of high-temperature plasmas. More practical applications include the MHD pump, MHD power generators and MHD devices used for stirring, levitating and controlling flows of liquid metals for metallurgical processes. Figure 1.2 below shows an example of an MHD generator.

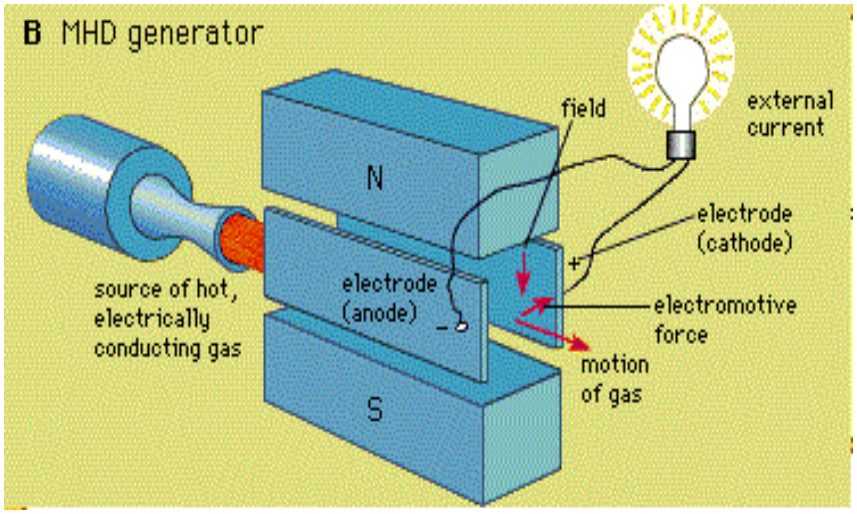

Figure 1.2: MHD generator (source: Encyclopedia Britannica)

1.3. Heat transfer

Heat transfer is the flow of thermal energy due to temperature differences and the subsequent temperature distribution and changes. Heat transfer is classified into modes such as thermal conduction, thermal radiation and thermal convection. Figure 1.3 below is a diagrammatic expression of the modes of heat transfer.

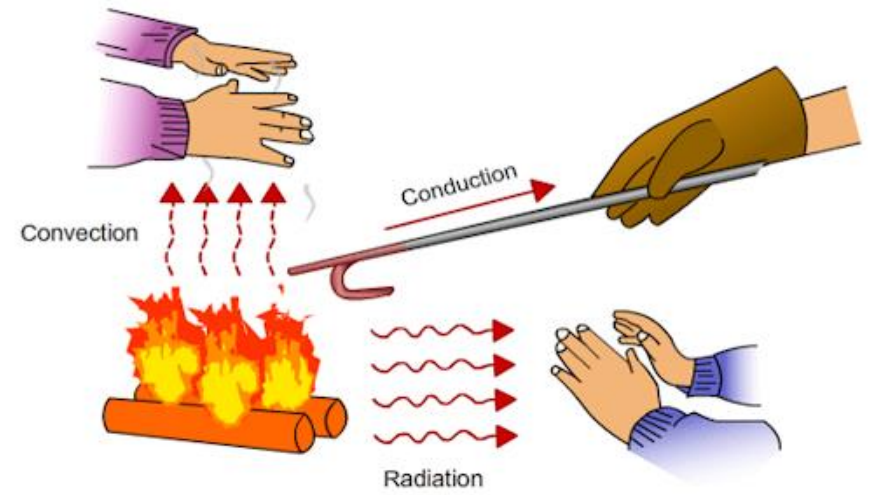

Figure 1.3: Modes of heat transfer. (source: www.onlinemech.com)

1.3.1. Thermal conduction

Thermal conduction also called diffusion is the exchange of kinetic energy of particles through the boundary between two systems. This flow of heat happens from a region of higher temperature to a region of a lower temperature until thermal equilibrium is attained. The quantity of heat transferred can be quantified using *Fourier's law*. The one-dimensional rate equation is given by

$$q_x'' = -k\frac{dT}{dx} \tag{1.1}$$

where k is the transport property known as the thermal conductivity and is a characteristic of a material in which conduction is taking place. The negative sign is due to the fact that heat is being transferred in the direction of decreasing temperature.

1.3.2. Thermal radiation

Thermal radiation is the emission of energy by matter that is at nonzero temperature. This energy is transferred through electromagnetic waves and happens through a vacuum. The energy emitted by a surface in form of radiation originates from the thermal energy of matter bounded by the surface. The rate at which energy is released is called the *emissive power E*, given by

$$E = \varepsilon\sigma T_s^4 \tag{1.2}$$

where ε is the radiative property of the material known as emissivity and σ is the Stefan-Boltzmann constant.

1.3.3. Thermal convection

Thermal convection occurs when the flow of fluid carries heat along with the flow of matter in the fluid. Depending on how the flow is initiated, convection can be classified as natural convection and forced convection. Natural convection occurs when heated fluids expand, become less dense and rise while the cold fluid moves down to occupy the space left by the hot risen fluids. This effect is called the buoyancy effect. Forced convection occurs when fluids are forced to move by mechanical means such as pump, fan suctions etc. natural convection heat transfer has diverse applications in electronic cooling, heat exchangers to name just a few.

1.4. Boundary layer

A boundary layer occurs when a fluid flows over a flat plate. The fluid particles make contact with the surface and become stationary. These particles tend to decrease the motion of particles in the adjoining fluid layer, which acts to retard the motion of particles in the next layer up to a distance $y = \delta$ (where y is the increasing distance from the surface and δ is the boundary layer thickness) where the effect becomes negligible. This retardation of fluid motion is due to shear stresses τ acting in planes that are parallel to the fluid velocity. The velocity of the fluid will increase until it approaches the free stream value u_∞ which is outside the boundary layer. Fluid flow on a flat surface is characterized by two distinct regions; a thin fluid layer which is the boundary layer in which u velocity gradients and shear stresses are large and a region beyond the boundary layer in which the velocity gradient and shear stresses are minimal (Frank P. Incropera et al, 2006). The boundary layer thickness δ, is the value y of for which $u = 0.99u_\infty$. Since it's more involved with the velocity of the fluid, this boundary layer can be termed as the **velocity boundary layer.** The manner in which the velocity component u varies with y through the boundary layer is called the **boundary layer velocity profile.**

1.4.1. Thermal boundary layer

This boundary layer develops when the fluid free stream temperature is different from the surface temperatures in which the fluid flows on. In this study, we consider a vertical heated plate in which the fluid flows past it. As the fluid particles come into contact with the plate, they attain thermal equilibrium at the plate's surface temperature. The heated particles exchange energy with those in the adjoining fluid layer which leads to a formation of a temperature gradient. This temperature gradient exists in the thermal boundary layer and its thickness δ_t is defined as the value of y for which the ratio

$$\frac{(T_w - T)}{T_w - T_\infty} = 0.99$$

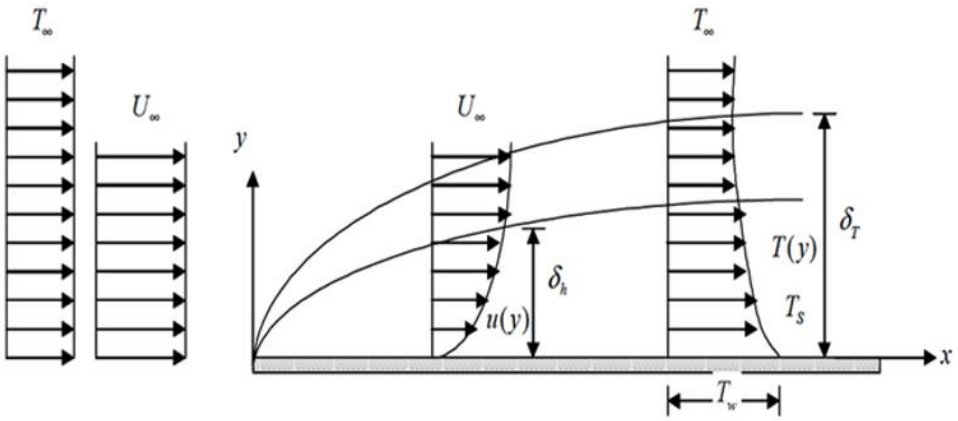

Figure 1.4: The Velocity and Thermal Boundary Layers(SM Seyedi 2019)

1.4.2. Concentration boundary layer

It occurs when the surface concentration of species is different from the free stream concentration. This is the region of the fluid in which the concentration gradient exists and the boundary thickness δ_c is defined as the value of y for which

$$\frac{(C_w - C)}{(C_w - C_\infty)} = 0.99$$

The conditions in the concentration gradient will influence the surface concentration gradient, the convection mass transfer which in turn affects the rate of species transfer in the boundary layer. Fig 1.5 shows the species concentration boundary layer development on a flat plate.

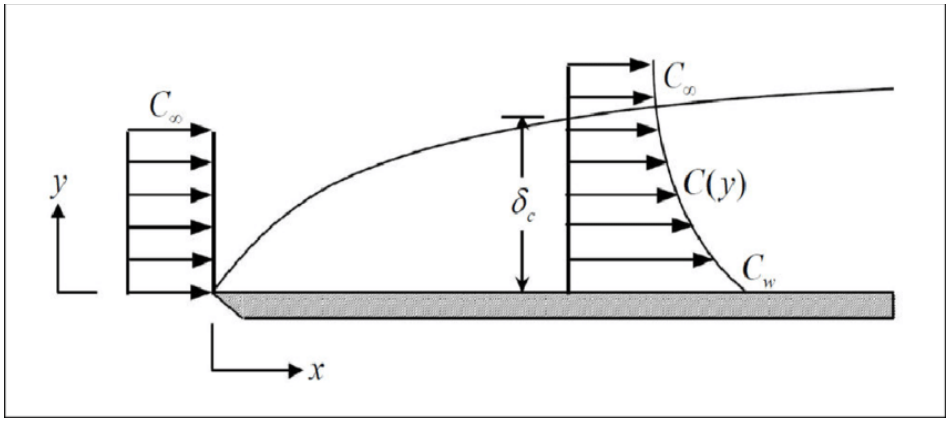

Figure 1.5: Concentration Boundary Layer(SM Seyedi 2019)

1.5. Mass transfer

This is the transport of mass in liquids or gaseous state due to differences in temperature, concentration or pressure gradients. Mass transfer can also take place due to chemical reactions where the flux of chemical species cannot be conserved since it's consumed and produced in a particular element. It can occur either in single-phase or multiphase systems. A fluid of chemical species travels from points of high concentration to low concentration. This flow of species can be described using the Fick's law which has the form

$$\dot{m} = -D_{AB}\ddot{M}a\frac{dC_A}{dy} \qquad (1.3)$$

Where $\dot{m}$ is the flow of substance A, $\ddot{M}$ the molecular weight of component A, D_{AB} is the binary diffusion coefficient of substance A in substance B and is determined by the physical properties of these substances. From the above, it can be concluded that mass transfer is analogous to heat transfer. When combined with heat transfer, mass transfer has wide industrial applications including metallurgy, power engineering and chemical processing equipments such as combustion chambers, fractionating towers absorbers and extractors and many more. In this study, we analyse the changes in the concentration gradient of the nanofluids. The particles in the fluid will diffuse as the liquid gets heated. If a fluid of species molar concentration C_∞ flows over a surface at which the species concentration is maintained at $C_w \neq C_\infty$, then the transfer of species will occur.

1.6. Viscous dissipation

Viscous dissipation is an irreversible process by which work done by a fluid on adjacent layers due to the action of shear forces is transformed into heat. This can also be stated as the conversion of kinetic energy into internal energy by work done against the viscous stresses and can be noted by a rise in temperature. Viscous dissipation changes the temperature distributions by playing a role like an energy source which affects heat transfer rates. Viscous dissipation is of interest in polymer processing flows such as injection molding or extrusion, condensation process of a metallic plate in a cooling bath among others.

1.7. Nanofluids

Most engineering and industrial processes occur at very high temperatures. To improve the performance of industrial machines, convectional fluids are used to facilitate the cooling process. The most commonly used conventional fluids are oil, water and ethylene glycol but

due to rising demand for fluids with higher heat dissipation properties, a certain class of fluid with an enhanced heat transfer technique called nanofluid was proposed. Nanofluid is a suspension of nanometer-sized particles (called nanoparticles) in a base fluid such as water, Ethylene Glycol, oil etc. Common nanoparticles include metals (such as Cu, Ag, Au etc.), oxide ceramics (such as Al_2O_3, CuO etc.), carbon nanotubes and carbide ceramics (such as SiC, Tic etc.). Nanofluids are good heat transmitters due to the presence of solid particles in the fluid and have a wide application including industrial coolants, microelectronics cooling, smart fluids and in the bio-medical sector (such as in nanocryosurgery).

1.8. The Shooting Technique

The shooting technique is a trial and error method used to convert a boundary value problem into an initial value problem. For the linear two-point boundary value problem, a system of two initial value problems is solved whose linear combination solves the boundary value problem. The IVPs are formed depending on the boundary conditions. The boundary value obtained is compared with the actual boundary value and using trial and error or some scientific approach, one tries to get as close to the boundary value as possible. Consider the two-point boundary value problem

$$y'' = f(x, y, y') \qquad y(a) = \alpha, \;\; y(b) = \beta \tag{1.4}$$

Whose unique solution is $y(x)$. using the shooting method, equation (1.4) is treated as an IVP in which x plays the role of the time variable, with a and b being the initial and final time respectively. The reduced IVP becomes

$$y'' = f(x, y, y') \qquad y(a) = \alpha, \;\; y'(a) = t \tag{1.5}$$

Where t must be chosen so that the solution satisfies the remaining boundary condition $y(b) = \beta$. Using the shooting technique, the boundary value problem is converted to an initial value problem and then solved using the fourth-order Runge-Kutta method.

1.9. The Fourth Order Runge-Kutta method

The Runge-Kutta fourth-order method is a numerical technique used to solve first order ordinary differential equations. Consider an initial value ordinary differential equations of the form

$$\frac{dy}{dx} = f(x, y) \qquad y(x_0) = y_0 \tag{1.6}$$

The fourth-order Runge-Kutta (RK4) scheme is given by

$$k_1 = hf(x_i, y_i), \qquad k_2 = hf\left(x_i + \frac{1h}{2}, y_i + \frac{1}{2}k_i\right), \tag{1.7a}$$

$$k_3 = hf\left(x_i + \frac{1}{2}h, y_i + \frac{1}{2}k_2\right), \qquad k_4 = hf(x_i + h, y_i + k_3), \tag{1.7b}$$

and

$$y_{i+1} = y_i + \frac{1}{6}(k_1 + 2k_2 + 2k_3 + k_4), \quad i = 0,1,\cdots,N-1. \tag{1.8}$$

Equation (1.7) is obtained from the first five terms of the Taylor series.

1.10. Statement of the Problem

This study shall investigate the effects of dissipative heat transfer on the magnetohydrodynamic flow of Copper (Cu) and Alumina (Al_2O_3) ethylene-glycol based nanofluid over a heated vertical plate. To unravel the dynamics of the flow extensively, effects of Lorentz force (induced by the magnetic field), viscous dissipation, mass transfer

and Brownian motion on the velocity profile, temperature profile, skin friction coefficient and local Nusselt number shall be investigated.

1.11. Justification of the study

Due to the growing demand and use of machines, the cooling of the machines has always been a great concern. Nanofluids have been greatly embraced to provide thermal solutions due to their special characteristics in viscosity, diffusivity, thermal conductivity and heat transfer capabilities. The choice of the base fluid is of importance as different fluids have different properties. Glycol based fluids always lower the freezing point of water and prevent ice formation and also raises the boiling point of water when mixed. This implies that the glycol-based fluids can be used both in the cooling systems like refrigeration and in the heating systems like the car radiators and the industrial heat exchangers (Sekrani 2018). In this study, nanometer-sized particles of Copper and Aluminum oxide have been combined with Ethylene Glycol as its base fluid. Based on the literature reviewed, it is clear that despite the numerous application of nanofluids, no author has investigated the effects of dissipative heat transfer for the magnetohydrodynamic flow of Copper (Cu) and Alumina (Al_2O_3) ethylene-glycol based nanofluid over a heated vertical plate.

1.12. Objectives

1.12.1 General objectives

The general objective of this study is to numerically analyse the effects of dissipative heat transfer on the hydromagnetic flow of Copper (Cu) and Alumina (Al_2O_3) Ethylene-Glycol based nanofluid on a heated vertical plate.

1.12.2 Specific objectives

The specific objectives of the study are to;

i. Formulate the partial differential equations governing the flow of nanofluid under the effects of magnetic field and viscous dissipation

ii. Analyse the effects of Eckert number, prandtl number, schimdt number, local biot number , magnetic field parameter, grashof number on;

(a) Velocity profile

(b) Temperature profile and

(c) Concentration profile

iii. Study the effects Eckert number, prandtl number, schimdt number, local biot number , magnetic field parameter, grashof number on;

(a) Skin friction

(b) Nusselt number and

(c) Sherwood number

1.13. Significance of the study

Owing to the increase in the demand for automobiles, the automotive industries are under a great challenge in designing automotive car frontal area and providing an engine which can be operated at high temperatures. With the advancement of nanotechnology, incorporating nanofluids as coolants will allow smaller size and better positioning of the car radiators leading to a better design in the frontal part of the car hence minimizing coefficient drag. This will translate into less fuel consumption and better performance of the engine since the use of ethylene-glycol based nanofluids will enable the engine to operate on very high temperatures.

Results obtained from this research shall also provide information for industries in enhancing industrial cooling of machines since a wide variety of industrial processes involve the transfer of heat energy. To achieve higher performance thermal systems, the use of nanofluids as coolants can be employed to achieve this. The high boiling point of ethylene glycol and good

thermal conductivity of the copper and aluminum oxide particles will enhance the cooling process hence saving the energy, reduce process time and consequently lengthen the working life of the machines.

Furthermore, the results will also come up with further insight into the use of nanofluids as coolants in electronics, transformers and in the medical field. Finally, further research can be carried out to further extend this study to a surface with a more complex geometrical structure.

CHAPTER TWO

LITERATURE REVIEW

Heat transfer has wide applications in our modern life. Combining the boundary layer flow with heat transfer has wide industrial applications such as the heat exchangers, creating interest in this area. In 2010 Makinde *et al.* analyzed the effects of thermal buoyancy on the laminar boundary layer about a vertical plate in a fluid under a convective surface boundary condition. It was noted that increasing the Prandtl number and the Grashof number leads to a reduction of the thermal boundary layer thickness along the plate. Desale *et al* (2015) did the numerical solution of boundary layer flow equation with viscous dissipation effect along a flat plate while considering varying temperature. It was observed that an increase in temperature leads to an increase in Eckert number while for a fixed Prandtl number and increase in Eckert number lead to a decrease in heat transfer at the wall. Basant *et al*. (2018) studied a mixed convection flow in a channel with temperature dependent viscosity and a flow reversal. They concluded that an increase in viscosity variation parameter increases both fluid velocity as well as the skin friction at the heated wall.

The influence of magnetic field on boundary layer flow has drawn the attention of some researchers. Lakshmi *et al*. (2013) did a numerical study of magnetohydrodynamic convection flow of heat and mass transfer past a plate considering viscous dissipation and internal heat generation. It was noted that velocity decreases with an increase in magnetic field strength, Schmidt number and Prandtl number. It was also concluded that the rate of heat transfer decreased with an increase in Prandtl number (Pr) and Eckert number while it increased in Schmidt number. Amami *et al*. (2014) carried out a numerical study of the effects of viscous dissipation on heat transfer, thermal energy storage by sensible heat and entropy generation within a porous channel with insulated walls subjected to a magnetic field.

He concluded that an increase in entropy generation was due to an increase in Eckert number and Hartmann number. External magnetic force was noted to affect the porous heat storage systems efficiency at a greater magnitude. Sivaiah (2013) studied the hydromagnetic flow of a rotating fluid past in the presence of chemical reaction and radiation. The flow was past a vertical plate and he considered the plate to be porous. He concluded that the concentration decreases with an increase in the chemical reaction parameter while the temperature increases with an increase with the radiation parameter

In the need of finding a fluid with better heat transfer abilities, Choi (1995) came up with a new class of heat transfer fluids called nanofluids which were obtained by suspending metallic nanoparticles in conventional heat transfer fluids termed as base fluids. It was concluded that the presence of the nanoparticles greatly leads to an increase in the heat transfer capabilities of the fluids. William *et al* (2006) proposed that Brownian motion had very little effect on the thermal conductivity of the nanofluid. Rehena *et al.* (2012) investigated the transient forced convection in a fluid valve filled with Copper Oxide-water nanofluid. Prandtl number was varied but the Reynolds number and solid volume fraction were fixed and concluded that the structure of the fluid flow and temperature field within the fluid valve depended significantly on time and the Copper oxide nanoparticles was most effective in enhancing heat transfer at the highest Prandtl value. Mohammed Uddin *et al* (2012) studied MHD laminar free convective boundary layer flows of an electrically conducting nanofluid over a solid stationary vertical plate. He concluded that there was an increase in the rate of heat and mass transfer and also an increase in the velocity and temperature distributions due to an increase in the Newtonian heating parameter. Jawad Raza *et al* (2016) did a numerical study of copper-water nanofluid through a stretching channel under slip effects considering different shapes of particles. The study revealed that the thermal boundary layer thickness increases by increasing the solid volume fraction. Vajravelu

et al. (2012) studied the effects of variable fluid properties on the boundary layer flow and heat transfer of a nanofluid over a horizontal surface where the effects of Brownian motion viscous dissipation and thermophoresis were considered. It was concluded that the effect of the Brownian motion and the thermophoresis parameters is to lower the wall-temperature gradient and to reduce the thickness of the nanoparticle volume fraction boundary layer for the case of Brownian motion parameter and to increase the thickness of the nanoparticle volume fraction boundary layer for the case of the Thermophoresis parameter.

Since there is an interaction of the magnetic field in most industrial processes, researchers decided to study the effects of applying magnetic field in a nanofluid flow. Makinde and Mutuku (2014) studied the effect of interaction between the electrical conductivity of the convectional base fluid and that of the nanoparticles under the influence of magnetic field in a boundary layer flow with heat transfer over a convectively heated flat surface, it was also observed that the presence of nanoparticles greatly enhances the magnetic susceptibility of nanofluids as compared to the base fluids. Khorasanizadeh *et al.* (2014) numerically investigated the heat transfer of variable properties of Alumina-Ethylene Glycol-water nanofluid in buoyancy driven convection where a rectangular plate was heated differently. The results were that as the volume fraction on nanoparticle increases deterioration in heat transfer occurred as compared to the base fluid heat transfer because of an increase in viscosity as the volume fraction of the nanoparticle increased. Mutuku (2014) analysed the hydromagnetic boundary layer flow and heat transfer of nanofluids and obtained that the presence of nanoparticles greatly enhanced the magnetic susceptibility of nanofluids as compared to the conventional based fluids. On increasing the magnetic strength of the fluid velocity was decreased while the thermal boundary layer thickness was increased hence an increase in the surface cooling effect. Zhao (2017) did a numerical study of electromagnetic flow and heat transfer characteristics of nanofluid inside a parallel plate microchannel. The

nanofluid was actuated by Lorentz force and the influence of viscous dissipation and joule heating was also considered. It was noted that an increase of the joule parameter and Brinkman number lead to a decrease in heat transfer performance while an increase in nanoparticle volume fraction leads to an increase in heat transfer capabilities.

This study aims to extend the work of Mutuku (2016) where the cooling capabilities of ethylene glycol (EG) based Nanofluid containing three different types of nanoparticles (i.e. copper oxide, aluminum oxide and titanium dioxide) was studied. It was concluded that the copper oxide ethylene glycol-based nanofluid lead to a faster decrease of temperature at the boundary layer as compared to aluminum oxide and titanium oxide ethylene glycol-based nanofluids. The aim was to compare heat transfer enhancement to base fluids due to the presence of different nanoparticles under the effect of the magnetic field. In this study, we study the dissipative heat transfer of hydromagnetic flow of Copper and Alumina over a heated vertical plate. We will consider the effect of mass transfer in the heat transfer abilities of the nanofluids. To the best of our knowledge, the present paper is the first to consider such a problem.

CHAPTER THREE

THE GOVERNING EQUATIONS

3.0. Introduction

In this chapter, we are to present the specific equations governing the flow of Copper and Aluminum oxide based nanofluid past a vertical plate in the presence of magnetic field while considering heat dissipation. The assumptions made in this study are stated. The general equations describing the flow are the continuity, momentum, energy and the concentration equation

3.1. Assumptions

The following assumptions are considered;

i. The flow is steady

ii. The fluid is incompressible

iii. The fluid has a two-dimensional flow

3.2. Specific Equations

A steady two-dimensional boundary layer flow of a nanofluid over a flat vertical plate is considered in this study. As shown in figure (3.1), the nanofluid flows across the vertical surface (i.e. x −axis) while a magnetic field of strength B_0 is applied normal to the surface. The surface is subjected to Newtonian heating boundary conditions.

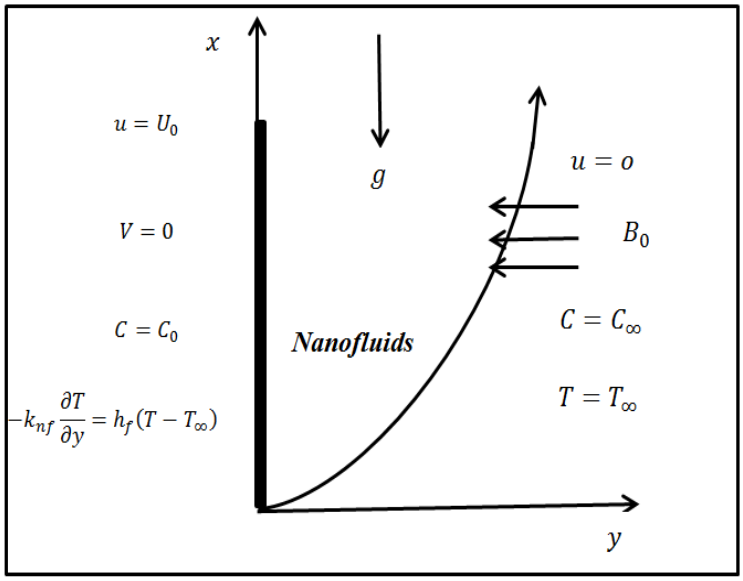

Figure 3.1: Flow configuration

3.2.1. The continuity Equation

The equation of continuity is based on the law of conservation of mass which states that matter can neither be created nor destroyed. For a steady two dimensional incompressible flow, the continuity equation is

$$\frac{\partial u}{\partial x}+\frac{\partial v}{\partial y}=0 \qquad (3.1)$$

3.2.2. The Momentum (Navier Stokes) Equation

The Navier stokes equation is derived from the Newton's second law of motion which states that the product of mass and acceleration is equal to the sum of external forces acting on a body. The external forces acting on the fluid element are the body forces (gravitational, electromagnetic) and the surface forces (pressure forces and the viscous forces). Since the nanofluid flows past a heated plate, heat will be transferred by convection and the fluid will experience the buoyancy force due to difference in temperatures. The application of magnetic field normal to the flow of the fluid will lead to Lorentz force. Therefore the momentum equation becomes

$$u\frac{\partial u}{\partial x}+v\frac{\partial u}{\partial y}=\frac{\mu_{nf}}{\rho_{nf}}\frac{\partial^2 u}{\partial y^2}+\beta_{nf}g(T-T_\infty)+\frac{1}{\rho}\vec{j}\times\vec{B} \tag{3.2}$$

According to ohms law

$$\vec{j}=\sigma\left(\vec{E}+\vec{V}\times\vec{B}\right)$$

Taking $\vec{E}$ to be negligible, then

$$\vec{j}=\sigma\left(\vec{V}\times\vec{B}\right)$$

Where $\vec{B}=\overrightarrow{B_o}+\vec{b}$. The quantity $\vec{b}$ is the magnetic induction resulting from the electric current $\vec{j}$ in the fluid. Since $\vec{b}$ can be considered as a perturbation hence negligible in this analysis, then

$$\vec{j}=\sigma\left(\vec{V}\times\overrightarrow{B_o}\right)$$

The Lorentz force can be obtained by

$$F=\frac{\sigma}{\rho}\left(\vec{V}\times\overrightarrow{B_o}\right)\times\overrightarrow{B_o}$$

According to Rossow (1958)

$$\frac{\sigma}{\rho}\left(\vec{V}\times\overrightarrow{B_o}\right)\times\overrightarrow{B_o}=-\frac{\sigma}{\rho}\left[\vec{V}\left(\overrightarrow{B_o}.\vec{B}_o\right)-\overrightarrow{B_o}\left(\overrightarrow{B_o}.\vec{V}\right)\right] \tag{3.3}$$

Since the magnetic field is applied normally to the flow, then

$$\overrightarrow{B_o}.\vec{V}=B_oVCos90=0$$

Therefore

$$F = -\frac{\sigma B_o^2}{\rho}\vec{V} \tag{3.4}$$

Substituting equation (3.4) into equation (3.2) while considering a two-dimensional flow, the momentum equation becomes

$$u\frac{\partial u}{\partial x} + v\frac{\partial u}{\partial y} = \frac{\mu_{nf}}{\rho_{nf}}\frac{\partial^2 u}{\partial y^2} + \beta_{nf} g(T - T_\infty) - \frac{\sigma_{nf} B_0^2 u}{\rho_{nf}} \tag{3.5}$$

Where the subscripts nf stand for nanofluids, μ represents the dynamic viscosity, ρ the density, β denotes the thermal expansion coefficient, B_o stands for magnetic field and σ stands for electrical conductivity of the nanofluid. Equation (3.5) can also be expressed as

$$u\frac{\partial u}{\partial x} + v\frac{\partial u}{\partial y} = \mathrm{U}_{nf}\frac{\partial^2 u}{\partial y^2} + \beta_{nf} g(T - T_\infty) - \frac{\sigma_{nf} B_0^2 u}{\rho_{nf}} \tag{3.6}$$

where $\mathrm{U}_{nf} = \frac{\mu_{nf}}{\rho_{nf}}$, μ_{nf} is the dynamic viscosity of the nanofluid and ρ_{nf} is the density of the nanofluid.

3.2.3. The Energy Equation

The energy equation is obtained from the principle of conservation of energy which is described by the first law of thermodynamics. In this study, viscous dissipation is considered since the fluid is highly viscous due to the presence of copper and aluminum oxide particles. Since the nanofluid is flowing under the influence of the magnetic field, the energy transfer

due to the magnetic effect will be considered. Therefore, for this flow, the energy equation will be expressed by

$$u\frac{\partial T}{\partial x}+v\frac{\partial T}{\partial y}=\frac{k_{nf}}{(\rho c_p)_{nf}}\frac{\partial^2 T}{\partial y^2}+\frac{\mu_{nf}}{(\rho c_p)_{nf.}}\left(\frac{\partial u}{\partial y}\right)^2+\frac{\sigma_{nf}B_o^2u^2}{(\rho c_p)_{nf}} \tag{3.7}$$

Where k stands for thermal conductivity and ρc_p refers to the heat capacitance of the fluid. The energy equation can be simplified further to be

$$u\frac{\partial T}{\partial x}+v\frac{\partial T}{\partial y}=\alpha_{nf}\frac{\partial^2 T}{\partial y^2}+\frac{\mu_{nf}}{(\rho c_p)_{nf.}}\left(\frac{\partial u}{\partial y}\right)^2+\frac{\sigma_{nf}B_o^2u^2}{(\rho c_p)_{nf}} \tag{3.8}$$

Where $\alpha_{nf}=\frac{k_{nf}}{(\rho c_p)_{nf}}$

3.2.4. The Concentration Equation

For a viscous liquid composed of a binary mixture, there will be a transport of species if there exist concentration gradients. Since the conservation of species must be satisfied at each point of the fluid, the processes affecting the transport of the species must be identified to obtain the conservation equation. The transport of species occurs by convection processes and diffusion. For this study, convective mass transfer is considered. This occurs when there is variation in density within the fluid phase caused by temperature differences or relatively large concentration differences. Therefore, the rate equation for convective mass transfer is given by

$$u\frac{\partial C}{\partial x}+v\frac{\partial C}{\partial y}=D_B\frac{\partial^2 C}{\partial y^2} \tag{3.9}$$

where D_B represents the Brownian diffusion coefficient.

According to Khorasanizadeh (2014), the following constant properties were validated experimentally by various researchers in relation between the nanofluid (*nf*), the base fluid (*bf*) and the nanoparticles (*np*). These relations can be used to determine the physical properties of nanofluids such as density, viscosity, specific heat, volume expansion and thermal conductivity at different temperatures and concentrations.

$$\rho_{nf} = (1-\varphi)\rho_{bf} + \varphi\rho_{np} \tag{3.10a}$$

$$\mu_{nf} = \frac{\mu_{bf}}{(1-\varphi)^{2.5}} \tag{3.10b}$$

$$\beta_{nf} = (1-\varphi)\beta_{bf} + \varphi\beta_{np} \tag{3.10c}$$

$$\left(\rho c_p\right)_{nf} = (1-\varphi)\left(\rho c_p\right)_{bf} + \varphi\left(\rho c_p\right)_{np} \tag{3.10d}$$

$$k_{nf} = \frac{k_{np} + 2k_{bf} - 2\varphi\left(k_{bf} - k_{np}\right)}{k_{np} + 2k_{bf} + \varphi\left(k_{bf} - k_{np}\right)} k_{bf} \tag{3.10e}$$

$$\sigma_{nf} = (1-\varphi)\sigma_{bf} + \varphi\sigma_{np} \tag{3.10f}$$

Since the flow of the nanofluid is over a stationary, flat heated vertical plate, its velocity will vary from the wall up to the free stream. The temperature and the concentration will also vary due to the heating of the plate. Therefore, the boundary conditions of this flow are

$$u(x,0) = U_0, \qquad v(x,0) = 0, \qquad -k_{nf}\frac{\partial T}{\partial y}(x,0) = h_f\left(T_f - T(x,0)\right)$$

$$C(x,0) = C_0$$

$$u(x,\infty) = 0, \qquad T(x,\infty) \to T_{\infty}, \qquad C(x,\infty) \to C_{\infty} \tag{3.11}$$

where C_w is the nanoparticle concentration at the wall, C_{∞} and T_{∞} are the ambient values of the nanoparticle concentration and the temperature respectively.

CHAPTER FOUR

METHODOLOGY

In this chapter, we will solve the specific equations obtained in chapter three. The four specific equations, which are in partial differential form, will be converted to nonlinear ordinary differential equations by non-dimensionalization. The resulting system of ordinary differential equations will be solved numerically using the fourth-order Runge-Kutta method together with the linear shooting technique.

4.1 Non-dimensionalization and similarity transformation

Non-dimensionalization aims to simplify the partial differential equations by reducing the number of parameters and rescaling the individual variables and as a result, generalize the system for easy numerical computations. In this analysis, the scaling down is done using the method of similarity solution proposed by Blasius (1908).

Introducing the stream function $\psi(x, y)$ such that the velocity components u and v are given by

$$u = \frac{\partial \psi}{\partial y}, \quad v = -\frac{\partial \psi}{\partial x} \tag{4.1}$$

where

$$\eta = \left(\frac{a}{\nu_{bf}}\right)^{\frac{1}{2}} y, \qquad \psi = \left(\sqrt{a\nu}\right) x f(\eta), \qquad \theta(\eta) = \frac{T - T_\infty}{T_w - T_\infty}, \tag{4.2}$$

$$\phi(\eta) = \frac{C - C_\infty}{C_w - C_\infty}$$

are the similarity variables used to transform equations (3.1), (3.6), (3.8), (3.9) into dimensionless form. Taking the partial of η and ψ with respect to x and y, we obtain

$$\frac{d\eta}{dy} = \left(\frac{a}{\upsilon_{nf}}\right)^{1/2}, \qquad \frac{\partial\psi}{\partial x} = \left(a\upsilon_{nf}\right)^{1/2} f, \tag{4.3}$$

$$\frac{\partial\psi}{\partial y} = \left(a\upsilon_{nf}\right)^{1/2} x \frac{df}{d\eta}\frac{d\eta}{dy} = axf'. \tag{4.4}$$

Putting equations (4.3) and (4.4) in equations (4.1), we obtain

$$u = \frac{\partial\psi}{\partial y} = axf', \qquad v = -\frac{\partial\psi}{\partial x} = -\left(a\upsilon_{nf}\right)^{1/2} f. \tag{4.5}$$

Taking the partial derivative of u with respect to y, we obtain

$$\frac{\partial u}{\partial y} = axf''\frac{d\eta}{dx} = ax\left(\frac{a}{\upsilon_{nf}}\right)^{1/2} f'' \tag{4.6}$$

Squaring equation (4.6)

$$\left(\frac{\partial u}{\partial y}\right)^2 = \frac{a^3x^2}{\upsilon_{nf}}(f'')^2 \tag{4.7}$$

Taking the second partial of u with respect to y

$$\frac{\partial^2 u}{\partial y^2} = ax\left(\frac{a}{\upsilon_{nf}}\right)^{1/2} f'''\frac{d\eta}{dy} = \frac{a^2x}{\upsilon_{nf}} f''' \tag{4.8}$$

Taking the partial of u and v with respect to x and y respectively

$$\frac{\partial u}{\partial x} = af', \qquad \frac{\partial v}{\partial y} = -\left(a\upsilon_{nf}\right)^{1/2} f' \frac{\partial \eta}{\partial y} = -af' \tag{4.9}$$

This shows that

$$\frac{\partial u}{\partial x} + \frac{\partial v}{\partial y} = af' - af' = 0$$

Momentum equation

Substituting equations (4.5) and (4.9) into the LHS of equation (3.6) and;

$$u\frac{\partial u}{\partial x} + v\frac{\partial u}{\partial y} = (axf')(af') - \left(a\upsilon_{nf}\right)^{1/2} f(ax)\left(\frac{a}{\upsilon_{nf}}\right)^{1/2} f''$$

$$= a^2 x(f')^2 - a^2 x f f'' \tag{4.10}$$

$$= a^2 x[(f')^2 - ff''] \tag{4.11}$$

Taking the RHS of equation (3.6) and taking $T - T_\infty = (T_w - T_\infty)\theta$

$$\upsilon_{nf}\frac{\partial^2 u}{\partial y^2} + \beta_{nf} g(T - T_\infty) - \frac{\sigma_{nf} B_0^2 u}{\rho_{nf}} = \upsilon_{nf}\frac{a^2 x}{\upsilon_{nf}} f''' + \beta_{nf} g(T_W - T_\infty)\theta - \frac{\sigma_{nf} B_0^2}{\rho_{nf}} axf'$$

$$= a^2 x\left[f''' + \frac{\beta_{nf} g(T_W - T_\infty)\theta}{a^2 x} - \frac{\sigma_{nf} B_0^2}{a\rho_{nf}} f'\right] \tag{4.12}$$

Combining equation (4.11) and (4.12)

$$a^2 x\left[f''' + \frac{\beta_{nf} g(T_W - T_\infty)\theta}{a^2 x} - \frac{\sigma_{nf} B_0^2}{a\rho_{nf}} f'\right] = a^2 x[(f')^2 - ff'']$$

$$f''' + \frac{\beta_{nf} g(T_W - T_\infty)\theta}{a^2 x} - \frac{\sigma_{nf} B_0^2}{a\rho_{nf}} f' + ff'' - (f')^2 = 0 \tag{4.13}$$

Taking

$$Gr = \frac{\beta_{nf} g(T_W - T_\infty)}{a^2 x}, \qquad M = \frac{\sigma_{nf} B_0^2}{a\rho_{nf}}$$

then equation (4.13) becomes

$$f''' + Gr\theta - Mf' + ff'' - (f')^2 = 0 \tag{4.14}$$

Energy equation

It is easy to see from equation (4.2) that

$$C = C_\infty + (C_w - C_\infty)\phi, \tag{4.15}$$

Differentiating equation (4.15) with respect to x and y;

$$\frac{\partial C}{\partial x} = 0, \tag{4.16a}$$

$$\frac{\partial C}{\partial y} = (C_w - C_\infty)\phi' \frac{d\eta}{dy} = \left(\frac{a}{\upsilon_{nf}}\right)^{1/2} (C_w - C_\infty)\phi' \tag{4.16b}$$

Differentiating equation (4.16b) with respect to y;

$$\frac{\partial^2 C}{\partial y^2} = \left(\frac{a}{\upsilon_{nf}}\right)^{1/2} (C_w - C_\infty)\phi'' \frac{d\eta}{dy}$$

$$= \left(\frac{a}{\upsilon_{nf}}\right)(C_w - C_\infty)\phi'' \tag{4.17}$$

It is easy to see from equation (4.2) that

$$T = T_\infty + (T_w - T_\infty)\theta \tag{4.18}$$

Differentiating equation (4.18) with respect to x and y

$$\frac{\partial T}{\partial x} = 0 \tag{4.19a}$$

$$\frac{\partial T}{\partial y} = (T_w - T_\infty)\theta' \frac{d\eta}{dy} = (T_w - T_\infty)\theta' \left(\frac{a}{\upsilon_{nf}}\right)^{1/2} \tag{4.19b}$$

Differentiating equation (4.19b) with respect to y

$$\frac{\partial^2 T}{\partial y^2} = \left(\frac{a}{\upsilon_{nf}}\right)^{1/2} (T_w - T_\infty)\theta'' \frac{d\eta}{dy} = \frac{a}{\upsilon_{nf}} (T_w - T_\infty)\theta'' \tag{4.20}$$

Taking the LHS of equation (3.8) and substituting equation (4.5), (4.19a), and (4.19b)

$$u\frac{\partial T}{\partial x} + v\frac{\partial T}{\partial y} = axf'(0) - \left(a\upsilon_{nf}\right)^{1/2} f\left(\frac{a}{\upsilon_{nf}}\right)^{1/2} (T_w - T_\infty)\theta' = -a(T_w - T_\infty)f\theta' \tag{4.21}$$

Taking the RHS of equation (3.8) and substituting equation (4.20), (4.7), (4.16b) and (4.19b)

$$\alpha_{nf}\frac{\partial^2 T}{\partial y^2} + \frac{\mu_{nf}}{(\rho c_p)_{nf.}}\left(\frac{\partial u}{\partial y}\right)^2 + \frac{\sigma_{nf} B_o^2 u^2}{(\rho c_p)_{nf}}$$

$$= \alpha_{nf}\frac{a}{\upsilon_{nf}}(T_w - T_\infty)\theta'' + \frac{\mu_{nf}}{(\rho c_p)_{nf.}}\frac{a^3 x^2}{\upsilon_{nf}}(f'')^2 + \frac{\sigma_{nf} B_o^2}{(\rho c_p)_{nf}} a^2 x^2 (f')^2 \tag{4.22}$$

Combining equation (4.21) and (4.22)

$$\alpha_{nf}\frac{a}{\upsilon_{nf}}(T_w - T_\infty)\theta'' + \frac{\mu_{nf}}{(\rho c_p)_{nf.}}\frac{a^3 x^2}{\upsilon_{nf}}(f'')^2 + \frac{\sigma_{nf} B_o^2}{(\rho c_p)_{nf}} a^2 x^2 (f')^2 + a(T_w - T_\infty)f\theta'$$

$$= 0 \tag{4.23}$$

Dividing equation (4.23) by $\left(\frac{a}{\upsilon_{nf}}\right)(T_w - T_\infty)$

$$\alpha_{nf}\theta'' + \frac{\mu_{nf}}{(\rho c_p)_{nf.}}\frac{a^2x^2}{(T_w - T_\infty)}(f'')^2 + \frac{\sigma_{nf}B_o^2}{(\rho c_p)_{nf}(T_w - T_\infty)}ax^2\mho_{nf}(f')^2 + \mho_{nf}f\theta' = 0 \quad (4.24)$$

Now, combining equation (3.10d) and (3.10e)

$$\alpha_{nf} = \frac{k_{nf}}{(\rho c_p)_{nf}} = k_{bf}\frac{\left[\frac{k_{np} + 2k_{bf} - 2\varphi(k_{bf} - k_{np})}{k_{np} + 2k_{bf} + \varphi(k_{bf} - k_{np})}\right]}{(1-\varphi)(\rho c_p)_{bf} + \varphi(\rho c_p)_{np}}$$

$$= \frac{k_{bf}}{(\rho c_p)_{bf}}\frac{\left[\frac{k_{np} + 2k_{bf} - 2\varphi(k_{bf} - k_{np})}{k_{np} + 2k_{bf} + \varphi(k_{bf} - k_{np})}\right]}{(1-\varphi) + \varphi\frac{(\rho c_p)_{np}}{(\rho c_p)_{bf}}} \quad (4.25)$$

This implies that

$$\alpha_{nf} = \alpha_{bf}A$$

where

$$A = \frac{\left[\frac{k_{np} + 2k_{bf} - 2\varphi(k_{bf} - k_{np})}{k_{np} + 2k_{bf} + \varphi(k_{bf} - k_{np})}\right]}{(1-\varphi) + \varphi\frac{(\rho c_p)_{np}}{(\rho c_p)_{bf}}}.$$

Hence substituting $\alpha_{nf} = \alpha_{bf}A$ into equation (4.24) and dividing through by α_{bf}, we have

$$A\theta'' + \frac{\mu_{nf}}{\alpha_{bf}(\rho c_p)_{nf.}}\frac{a^2x^2}{(T_w - T_\infty)}(f'')^2 + \frac{\sigma_{nf}B_o^2}{(\rho c_p)_{nf}(T_w - T_\infty)\alpha_{bf}}ax^2\mho_{nf}(f')^2 + \frac{\mho_{nf}}{\alpha_{bf}}f\theta' = 0. \quad (4.26)$$

But

$$\frac{\sigma_{nf}B_o^2 a x^2 \mathrm{U}_{nf}}{(\rho c_p)_{nf}(T_w - T_\infty)\alpha_{bf}} = \frac{\sigma_{nf}B_o^2}{a\rho_{nf}} \times \frac{a^2x^2}{\left(c_p\right)_{nf}(T_w - T_\infty)} \times \frac{\mathrm{U}_{nf}}{\alpha_{bf}} = M \times Ec \times Pr$$

and

$$\frac{\mu_{nf}}{\alpha_{bf}(\rho c_p)_{nf.}} \frac{a^2x^2}{(T_w - T_\infty)} = \frac{\mathrm{U}_{nf}}{\alpha_{bf}} \times \frac{a^2x^2}{\left(c_p\right)_{nf}(T_w - T_\infty)} = Pr \times Ec \tag{4.28}$$

Substituting equation (4.27) and (4.28) into equation (4.26) we obtain;

$$A\theta'' + PrEc(f'')^2 + MEcPr(f')^2 + Pr\theta' = 0 \tag{4.29}$$

Concentration equation

Taking the LHS of equation (3.9) and substituting equation (4.5a), (4.16a), (4.5b) and (4.16b) respectively

$$u\frac{\partial C}{\partial x} + v\frac{\partial C}{\partial y} = axf'(0) - \left(a\mathrm{U}_{nf}\right)^{1/2} f\left(\frac{a}{\mathrm{U}_{nf}}\right)^{1/2}(C_w - C_\infty)\phi'$$

$$= -a(C_w - C_\infty)f\phi' \quad (4.30)$$

Taking the RHS of equation (3.9) and substituting equation (4.17) and (4.20)

$$D_B\frac{\partial^2 C}{\partial y^2} = D_B\left(\frac{a}{\mathrm{U}_{nf}}\right)(C_w - C_\infty)\phi'' \tag{4.31}$$

Combining equation (4.30) and (4.31);

$$D_B\left(\frac{a}{\mathrm{U}_{nf}}\right)(C_w - C_\infty)\phi'' + a(C_w - C_\infty)f\phi' = 0 \tag{4.32}$$

Dividing equation (4.32) by $D_B\left(\frac{a}{\mathrm{U}_{nf}}\right)(C_w - C_\infty)$, we obtain;

$$\phi'' + \frac{\mathrm{U}_{nf}}{D_B}f\phi' = 0$$

$$\phi'' + Scf\phi' = 0 \qquad (4.33)$$

where

$$Sc = \frac{\upsilon_{nf}}{D_B}.$$

Boundary conditions

It is clear that $y = 0$ implies that

$$\eta = \left(\frac{a}{\upsilon_{nf}}\right)^{1/2} \times 0 = 0$$

And since $u = U_w = ax$ at $y = 0$ then

$$axf' = ax \;\Rightarrow\; f' = 1, \qquad (\text{since } u = axf').$$

and comparing $v = 0$ with equation (4.5b), we have

$$f = 0.$$

Substituting equation (4.19b) into the condition

$$-k_{nf}\frac{\partial T}{\partial y} = h_f(T - T_{(x,0)})$$

we obtain

$$\theta' = \frac{h}{k_{nf}}\left(\frac{\upsilon_{nf}}{a}\right)^{1/2}(\theta - 1) = Bi(\theta - 1) \;\text{ where }\; Bi = \frac{h}{k_{nf}}\left(\frac{\upsilon_{nf}}{a}\right)^{1/2}.$$

Since $C(x,0) = C_0$ and $\phi(\eta) = \frac{C - C_\infty}{C_w - C_\infty}$, then at $\eta = 0, \qquad \phi = 1$

Consider $y \to \infty$, then $\eta \to \infty$ and

$$u \to 0 \;\Rightarrow f' \to 0,$$

$$T \to T_\infty \;\Rightarrow \theta \to 0,$$

$$C \to C_\infty \Rightarrow \phi \to 0$$

The resulting boundary dimensionless boundary conditions are

$$\text{at } \eta = 0;\ \ f' = 1,\ \ f = 0,\ \ \theta' = Bi(\theta - 1),\ \ \phi = 1$$

$$\text{as } \eta \to \infty;\ \ f' = 0, \qquad \theta \to 0, \qquad \phi \to 0$$

The non-dimensionalized equations are;

$$\boldsymbol{f''' + Gr\theta - Mf' + ff'' - (f')^2 = 0} \tag{4.34}$$

$$\boldsymbol{A\theta'' + PrEc(f'')^2 + MEcPr(f')^2 + Pr\theta' = 0} \tag{4.35}$$

$$\boldsymbol{\phi'' + Scf\phi' = 0} \tag{4.36}$$

with the boundary conditions as

$$\boldsymbol{\text{at } \eta = 0;\ \ f' = 1,\ \ f = 0,\ \ \theta' = Bi(\theta - 1),\ \ \phi = 1} \tag{4.37}$$

$$\boldsymbol{\text{as } \eta \to \infty;\ \ f' = 0, \qquad \theta \to 0, \qquad \phi \to 0} \tag{4.38}$$

where

$$Gr = \frac{\beta_{nf} g(T_W - T_\infty)}{a^2 x}, M = \frac{\sigma_{nf} B_0^2}{a\rho_{nf}}, Pr = \frac{\mathrm{U}_{nf}}{\alpha_{bf}}, Ec = \frac{a^2 x^2}{\left(c_p\right)_{nf}(T_w - T_\infty)},$$

$$, Sc = \frac{\mathrm{U}_{nf}}{D_B}, Bi = \frac{h}{k_{nf}}\left(\frac{\mathrm{U}_{nf}}{a}\right)^{1/2}$$

where Gr, M, Pr, Ec, Bi and Sc are the Grashof Number, Magnetic field Parameter, Prandtl Number, Eckert Number, Local Biot Number and the Schmidt Number respectively. The above set of non-dimensionalized equations together with their boundary conditions will analysed using the fourth-order Runge-Kutta method using the MATLAB software.

The following thermophysical properties will be useful in the analysis of our model equations as obtained from Mutuku (2016).

Table 1:Thermophysical properties of Ethylene-Glycol and Copper and Alumina nanoparticles

Materials	Density ρ (kg/m^3)	Specific heat at constant pressure c_p (J/kgK)	Thermal conductivity k (W/mK)	Electrical conductivity σ (S.m^{-1})	Thermal expansion coefficients β(K^{-1})	Dynamic Viscosity μ (pa.s)
Ethylene-glycol	1114	2415	0.252	1.07×10^{-6}	6.5×10^{-5}	0.0161
Alumina (Al_2O_3)	3970	765	40	3.69×10^{7}	0.85×10^{-5}	_
Copper (Cu)	8933	385	401	5.96×10^{7}	1.67×10^{-5}	_

CHAPTER FIVE

RESULTS AND DISCUSSION

This chapter is divided into three sections. In the first section, the effects of various thermophysical parameters on velocity, temperature and concentration profiles as well as the skin friction and the local Nusselt number are considered. The second section involves the conclusion of the study based on the results obtained and the last part is the recommendation.

5.1. Effects of various thermophysical parameters on the dynamics of the flow

The importance of this section is to analyse the effects of various thermophysical parameters on velocity, temperature and concentration profiles as well as the skin friction and the local Nusselt number. These parameters are the local Biot number, the Magnetic field parameter, the Schmidt number, the Eckert number, the Grashof number and the Prandtl number. The results are presented graphically in figures 5.1-5.20 followed by a detailed discussion and interpretation of the graphs.

5.1.1. Dimensionless velocity profiles

Figures 5.1- 5.12 show the effects of various physical parameters on the primary and the secondary velocity profiles of the nanofluids. For the case of the primary velocity, it is noted that the velocity is maximum at the plate surface but gradually decreases to zero at the ambient area far away from the plate with regards to all pertinent parameters, thus satisfying the boundary conditions. Consequently, the secondary velocity is observed to increase gradually from zero close to the plate attaining a maximum velocity at the free stream. In figure 5.1, an increase in the magnetic parameter leads to a decrease in the fluid velocity. This is due to an increase in the Lorentz force, a resistive force which tends to retard the motion of the fluid. However, the increase in Magnetic parameter showed an increase in the secondary velocity profileas displayed in fig 5.2. An increase in the viscous dissipation

parameter (Ec), leads to an increase in the velocity of the fluid as shown in figure 5.3. The velocity boundary layer thickness slightly increased due to an increase in the local Biot number as depicted in fig 5.5 due to convective heat transfer from the plate surface. Figure 5.11 shows the effects of increasing Grashof number on velocity profiles. Grashof number is the ratio between the buoyancy forces caused by changes in the fluid's density to the viscous force due to the restraining force caused by the viscosity of the fluid. An increase in the Grashof number results in the increase in velocity due to buoyancy forces.

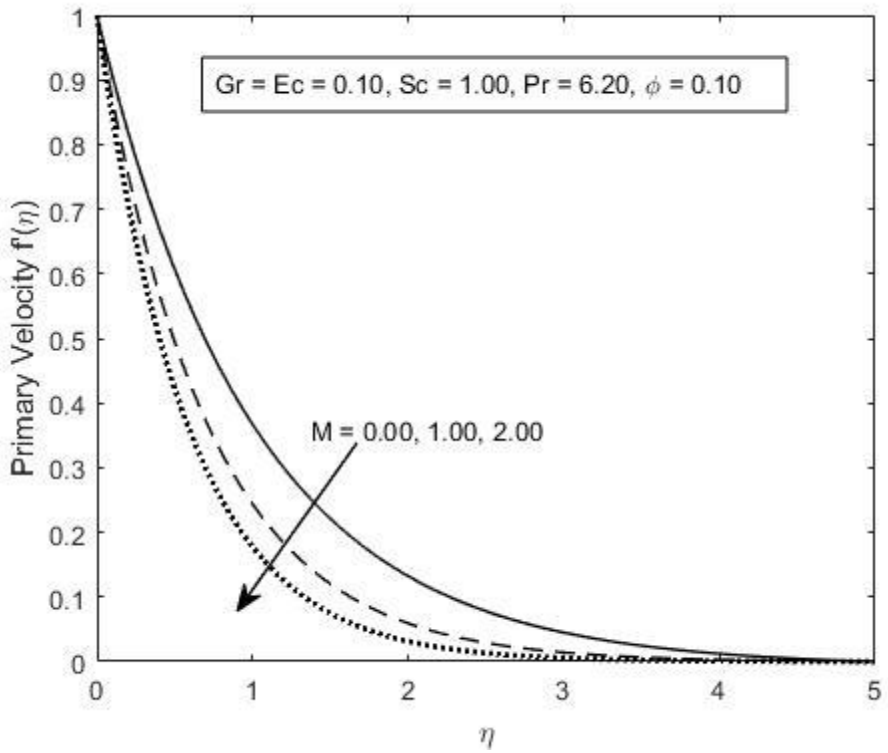

Figure 5.1: Primary Velocity profile for increasing Magnetic field Parameter

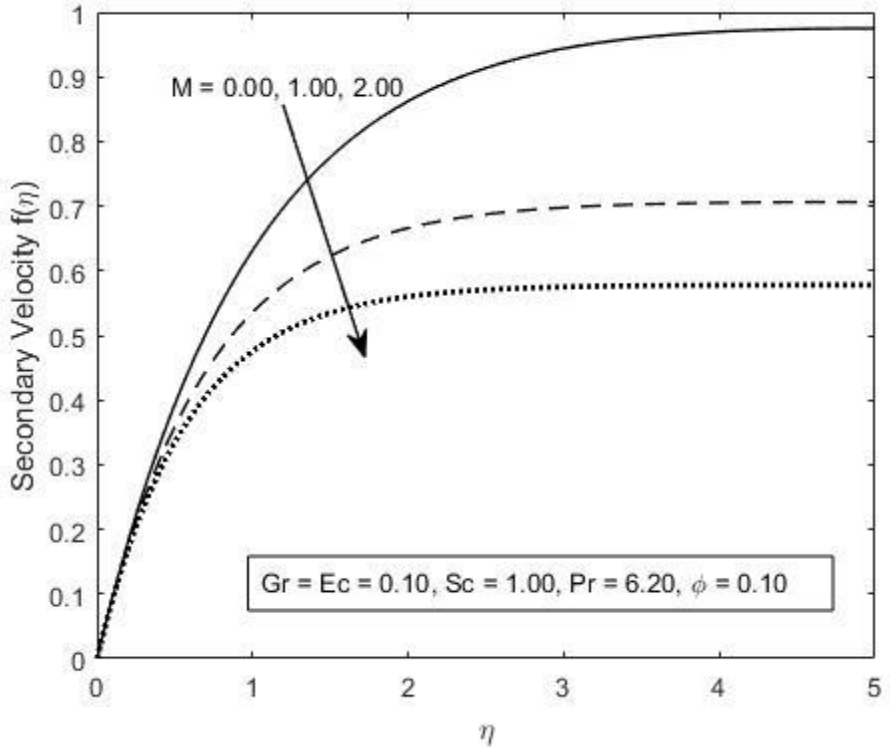

Figure 5.2: Secondary Velocity Profile for increasing Magnetic field Parameter

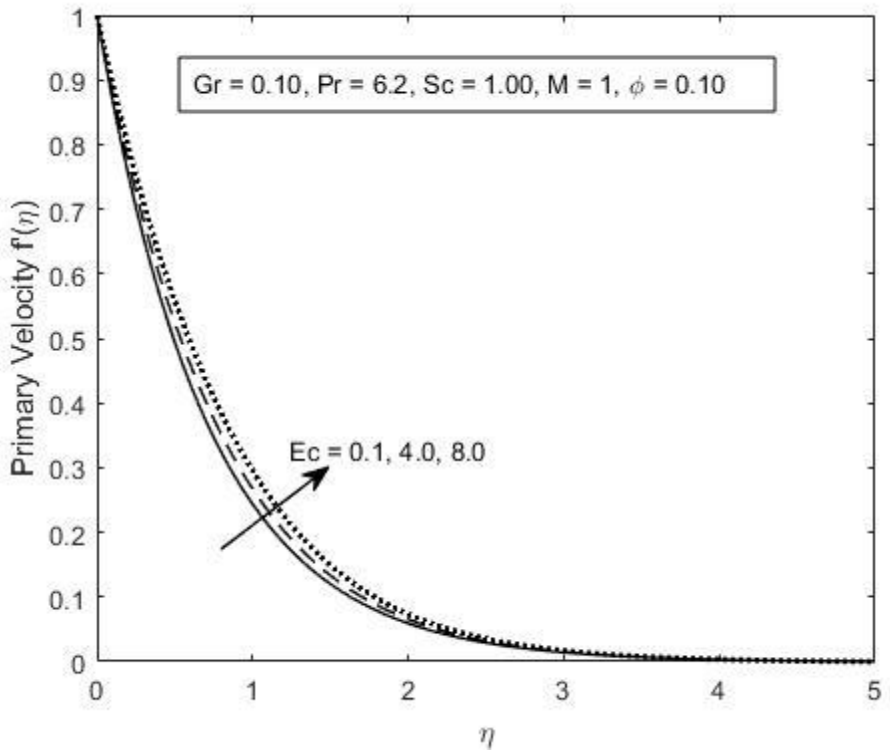

Figure 5.3: Primary Velocity Profile for increasing Eckert number

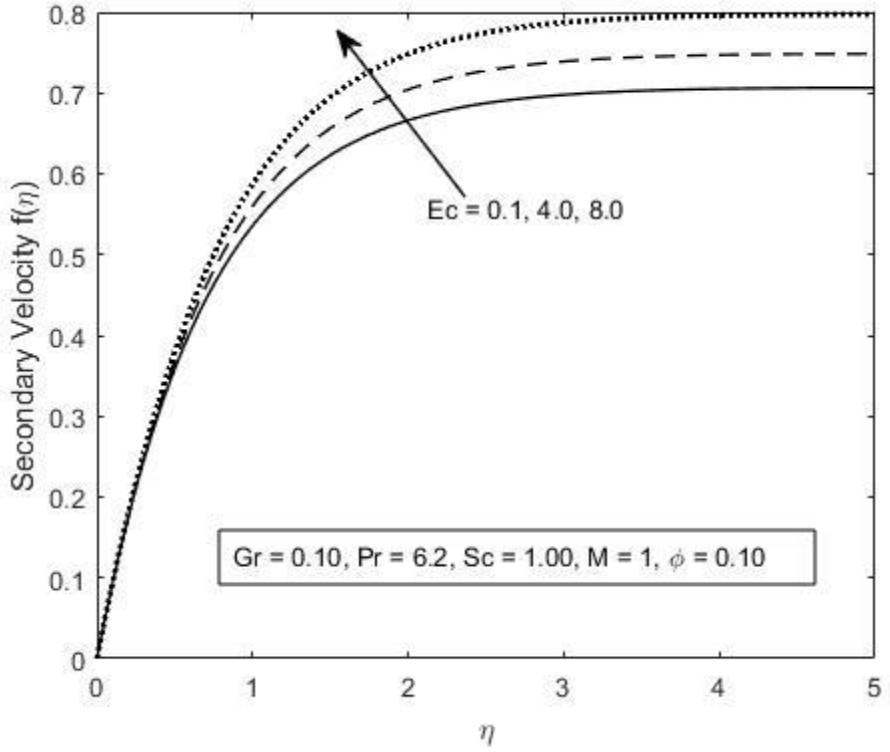

Figure 5.4: Secondary Velocity Profile for increasing Eckert number

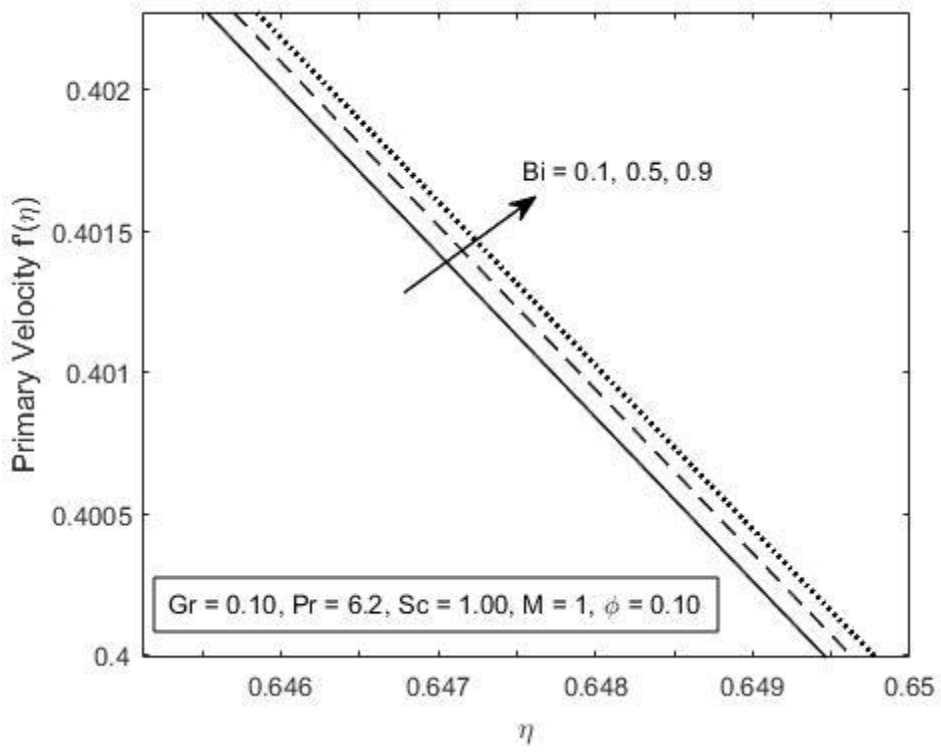

Figure 5.5: Primary Velocity Profile for Increasing Local Biot number

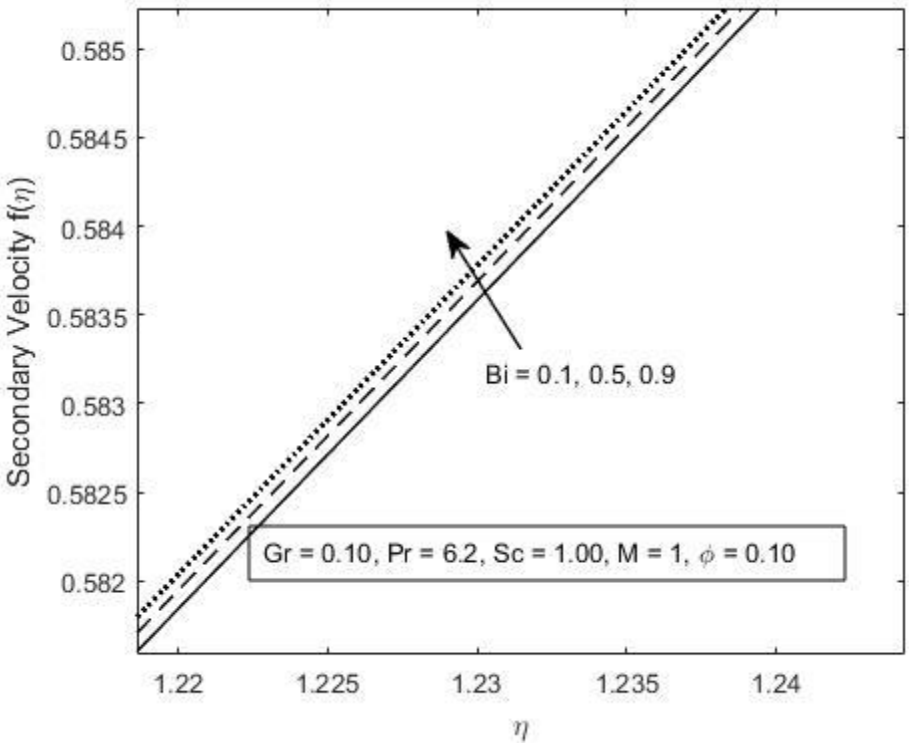

Figure 5.6: Secondary Velocity Profile for increasing Local Biot number

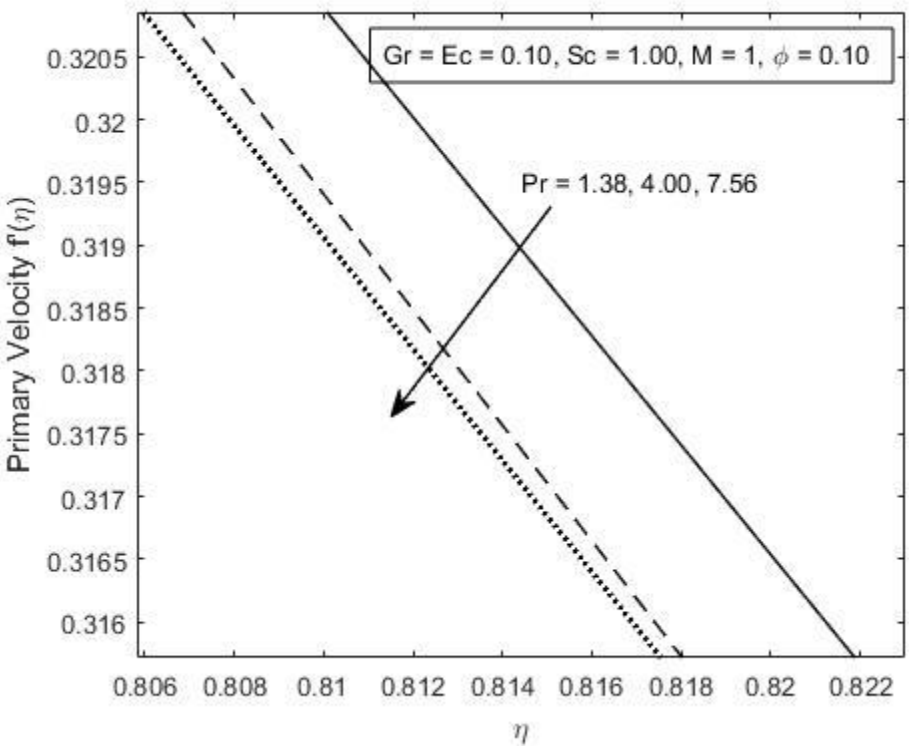

Figure 5.7: Primary Velocity Profile for increasing Prandtl number

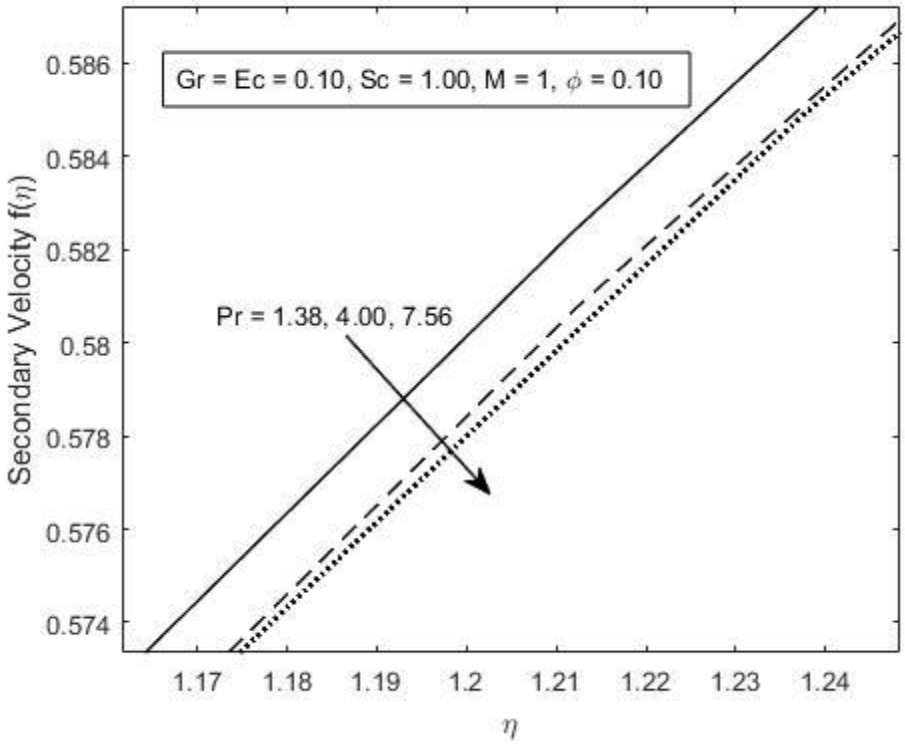

Figure 5.8: Secondary Velocity profile for increasing Prandtl number

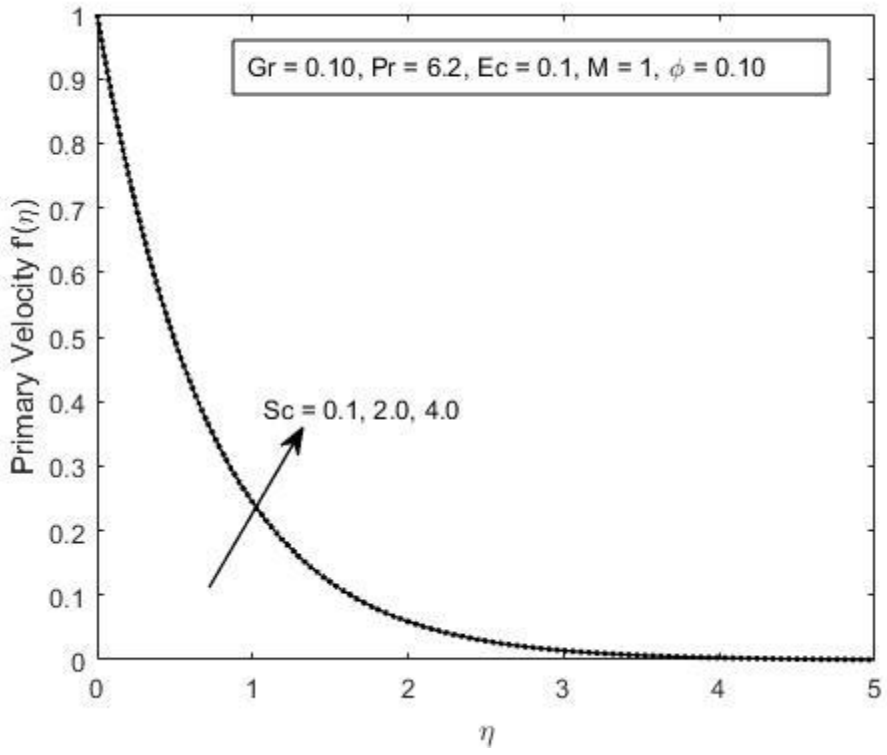

Figure 5.9: Primary Velocity Profile for increasing Schmidt number

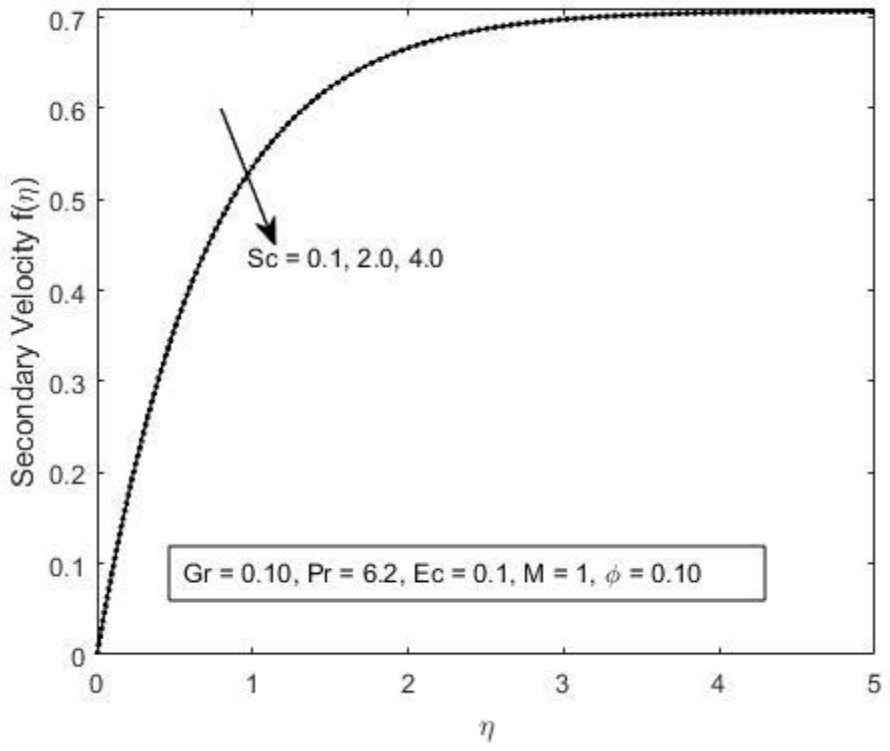

Figure 5.10: Secondary Velocity Profile for increasing Schmidt number

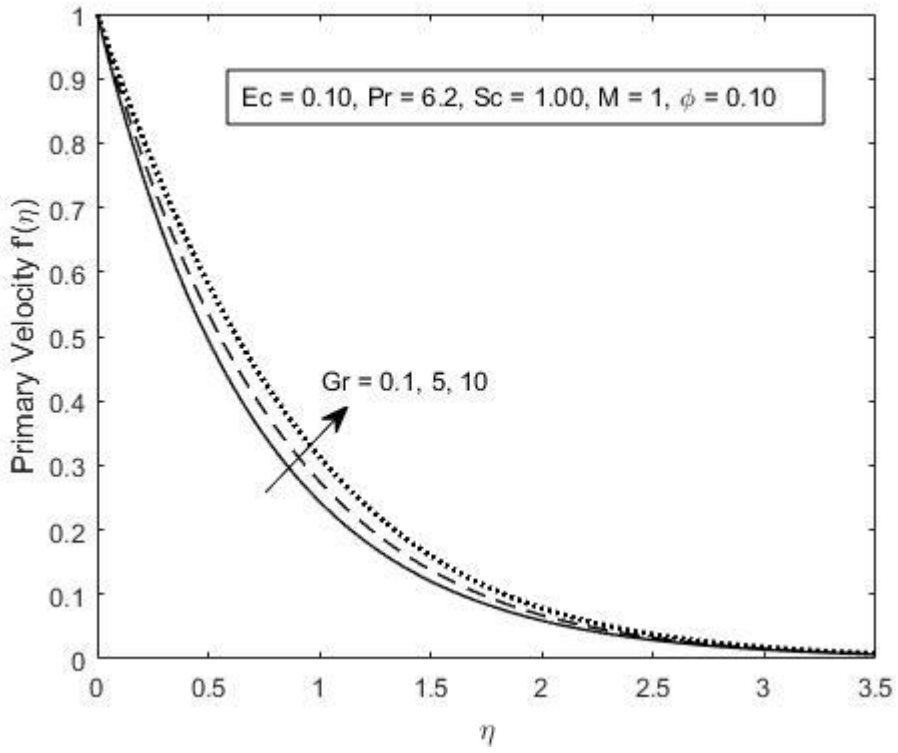

Figure 5.11: Primary velocity profile for increasing Grashof number

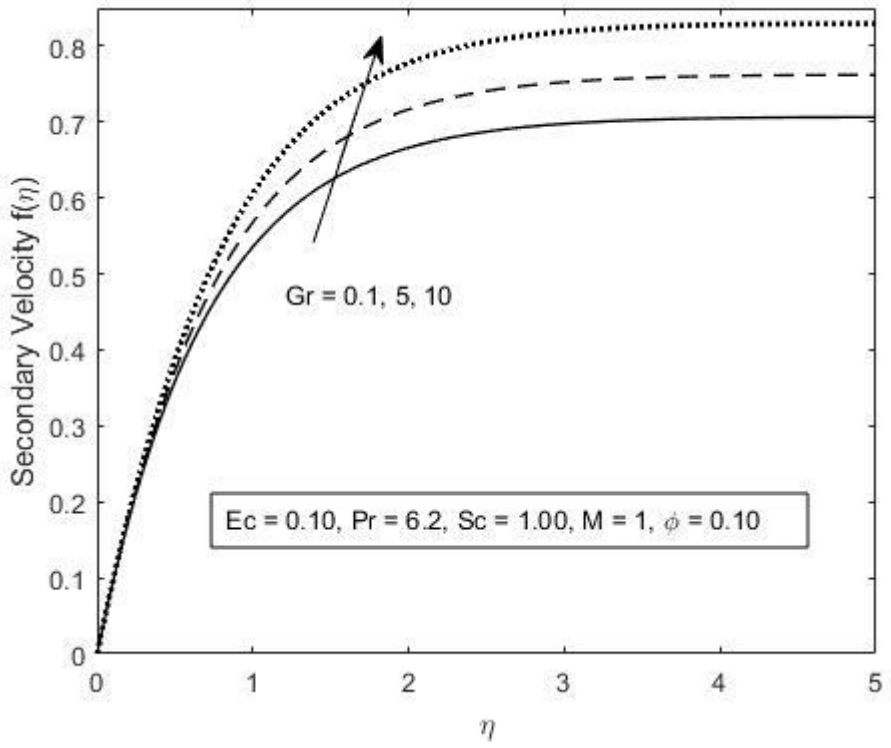

Figure 5.12: Secondary velocity profile for increasing Grashof number

5.1.2. Dimensionless Temperature Profiles

Figures 5.13-5.17 illustrates the fluid temperature profiles within the boundary layer. It can be observed that the fluid temperature is highest at the plate surface and decreases exponentially to zero at the free stream area far away from the plate satisfying the boundary conditions. From these figures, the thermal boundary layer thickness increases with an increase in the Magnetic field parameter, Eckert number and the local Biot number while it decreases with an increase in the Prandtl number. The Schmidt number has very little influence in the thermal boundary thickness. An increase in Magnetic parameter would result in an increase in the induced Lorentz force which will lead to resistance to the flow of the fluid as discussed in fig 5.1. Consequently this will increase the temperature as depicted in fig 5.13. An increase in the local Biot number leads to an increased rate at which heat is transferred between the hot plate and the fluid while an increase in Eckert number results in increase in temperatures due to the additional heating caused by the viscous dissipation. This

is displayedin fig 5.14 and fig 5.15 respectively. Fig 5.16 show the effect of varying prandtl number on temperature profile. Since the Prandtl number is the ratio of viscous diffusion to thermal diffusion, an increase in Prandtl number would result in a decrease in the thermal boundary layer thickness hence a decrease in the temperature. It can be observed in fig 5.17 that changes in Schmidt number have no effects on the temperature profile. Figure 5.18 shows the variation of the Grashof number to the temperature profiles. An increase in Grashof number reduces the thermal boundary layer but at the free stream, the temperature is seen to rise with an increase in Grashof number.

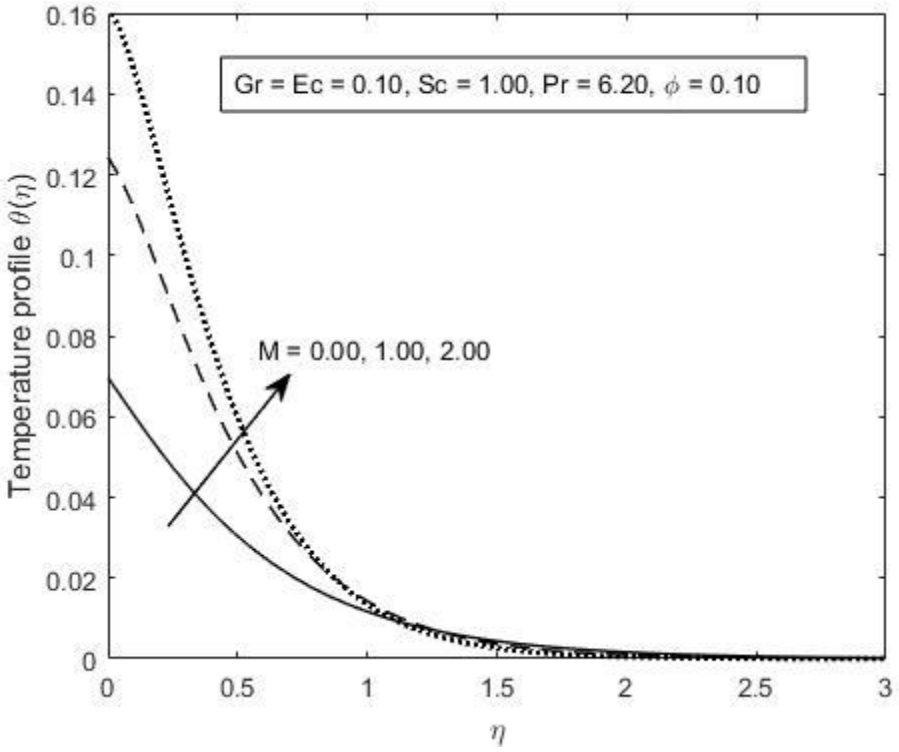

Figure 5.13: Temperature profile with increasing Magnetic Field Parameter

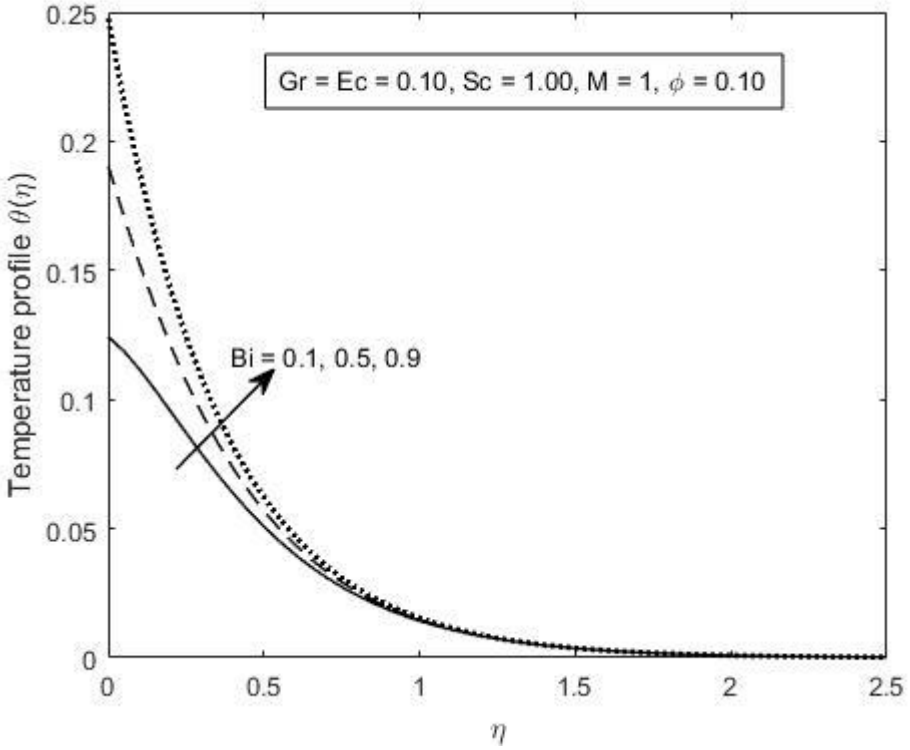

Figure 5.14: Temperature profile for increasing Local Biot number

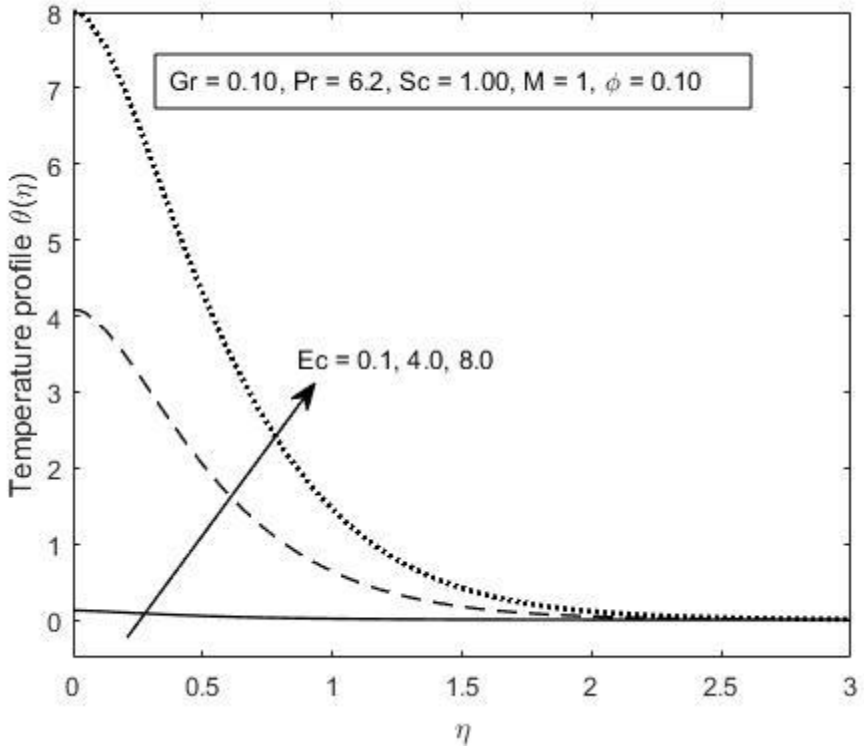

Figure 5.15: Temperature profile for increasing Eckert number

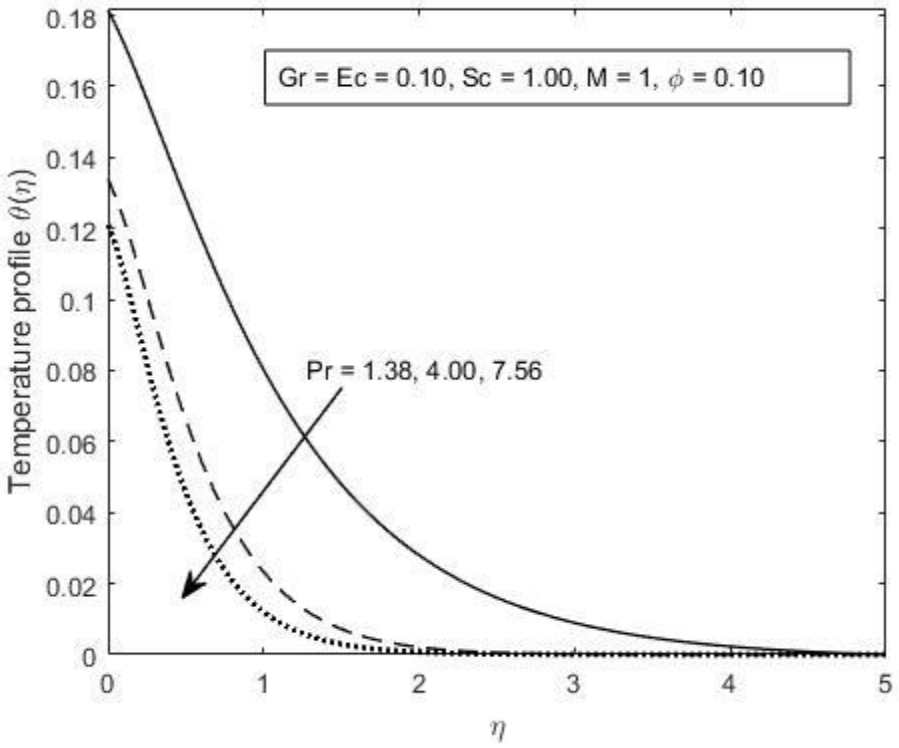

Figure 5.16: Temperature Profile for increasing Prandtl number

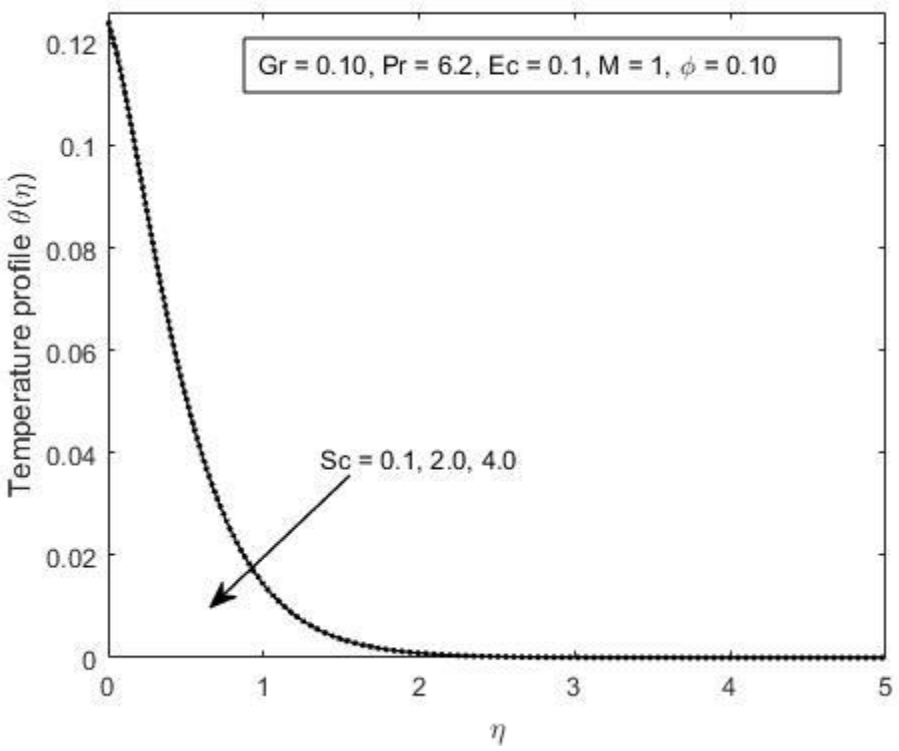

Figure 5.17: Temperature Profile for increasing Schmidt number

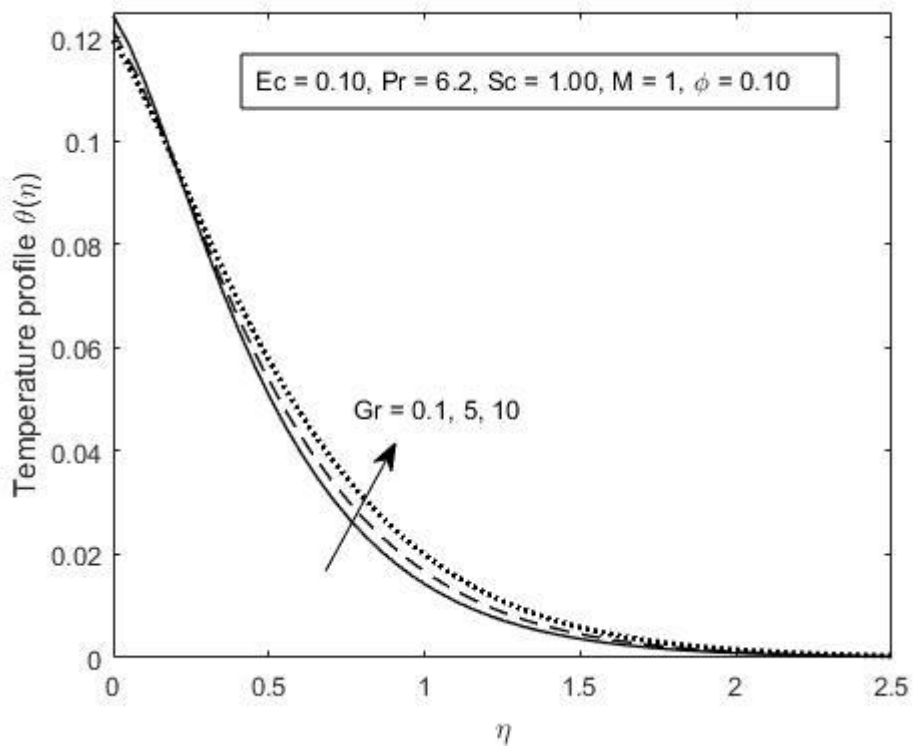

Figure 5.18: Temperature Profile for increasing Grashof number

5.1.3. Dimensionless Concentration Profiles

Fig 5.19- 5.24 shows the concentration profiles against the spanwise coordinate η for varying values of Magnetic parameter, Eckert number, Local Biot number, Prandtl number, Schmidt number and the Grashof number. The species concentration is seen to decrease to zero from the late surface up to a region far away from the plate, thus satisfying the boundary conditions. From these figures, it can be noted that varying the magnetic field parameter and the Schmidt number has a great influence on the concentration boundary layer while changes in the Local Biot number and the Eckert number have very little effect on the species concentration gradient. Fig 5.19 shows that increasing the Magnetic field parameter leads to an increase in the concentration gradient. This is due to the resistive force induced which will in turn reduce the velocity and subsequently increase the temperature of the fluid. Fig 5.20 shows variation of Eckert number on the concentration profile. It shows that an increase in the temperature of the fluid will increase the diffusion coefficient of the nanofluids hence

increase in the concentration gradient. Fig 5.21 and fig 5.22 shows that there is very little effect of the local biot number and prandtl number on the concentration profile. Fig 5.23 depicts that an increase in Schmidt number leads to a decrease in concentration due to a weaker solute diffusivity leading to a shallower penetration of solutal effect. Figure 5.24 shows that an increase in the Grashof number would result in a decrease in the concentration. This is because an increase in buoyancy forces leads to a further dispersion of the concentration species.

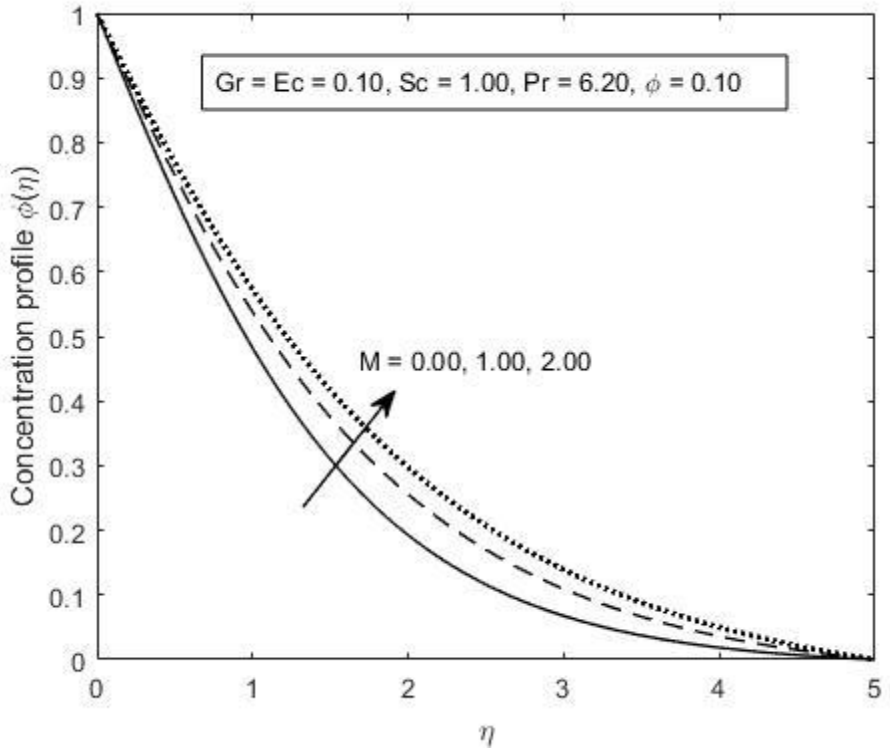

Figure 5.19: Concentration profile for increasing Magnetic Field Parameter

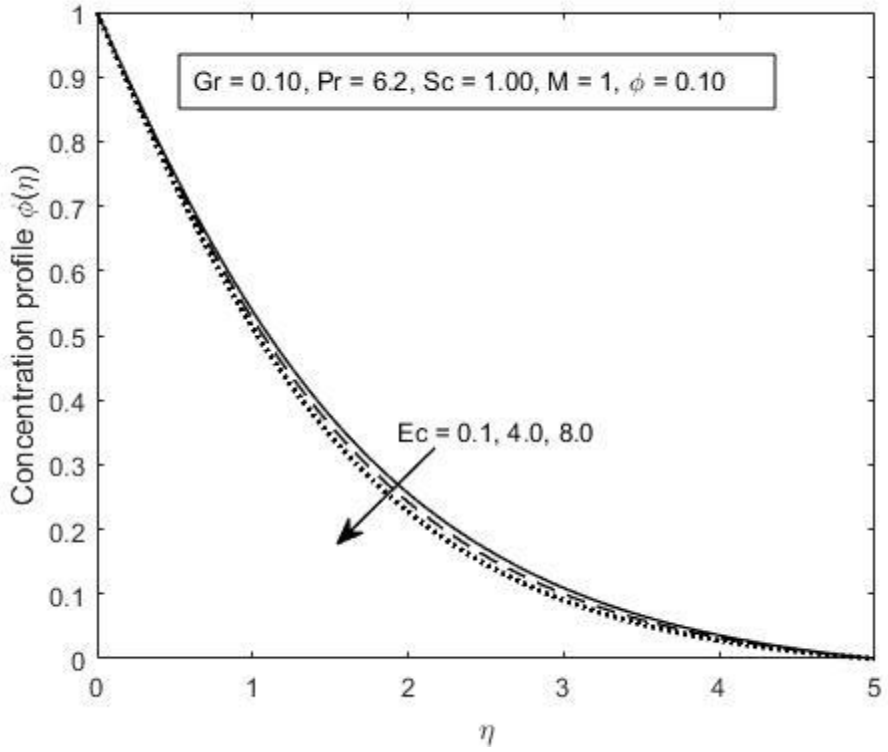

Figure 5.20: Concentration Profile with increasing Eckert number

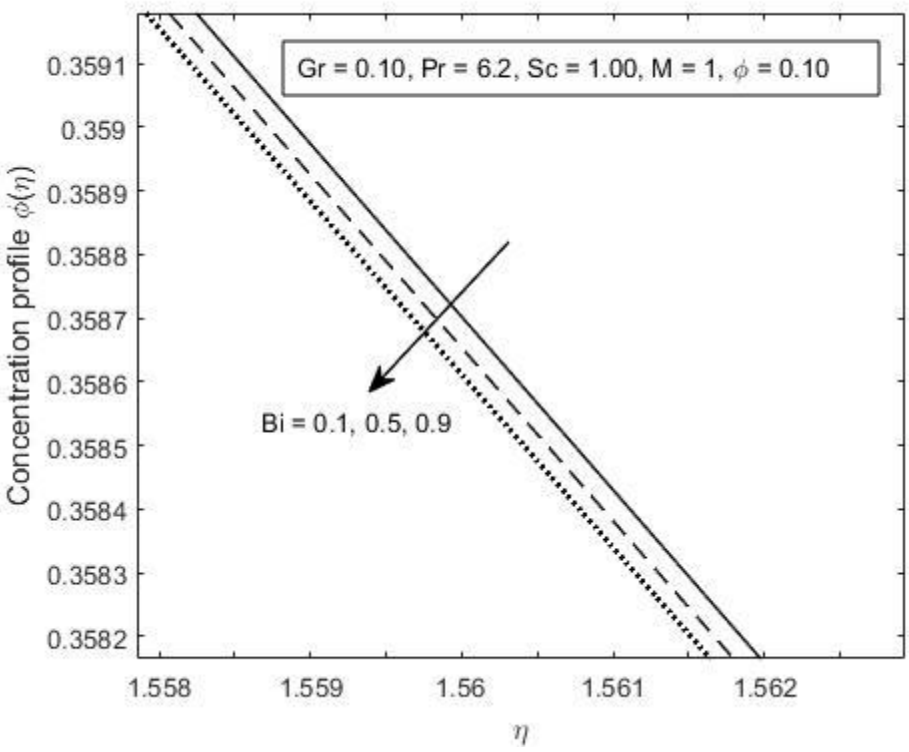

Figure 5.21: Concentration Profile for increasing Local Biot number

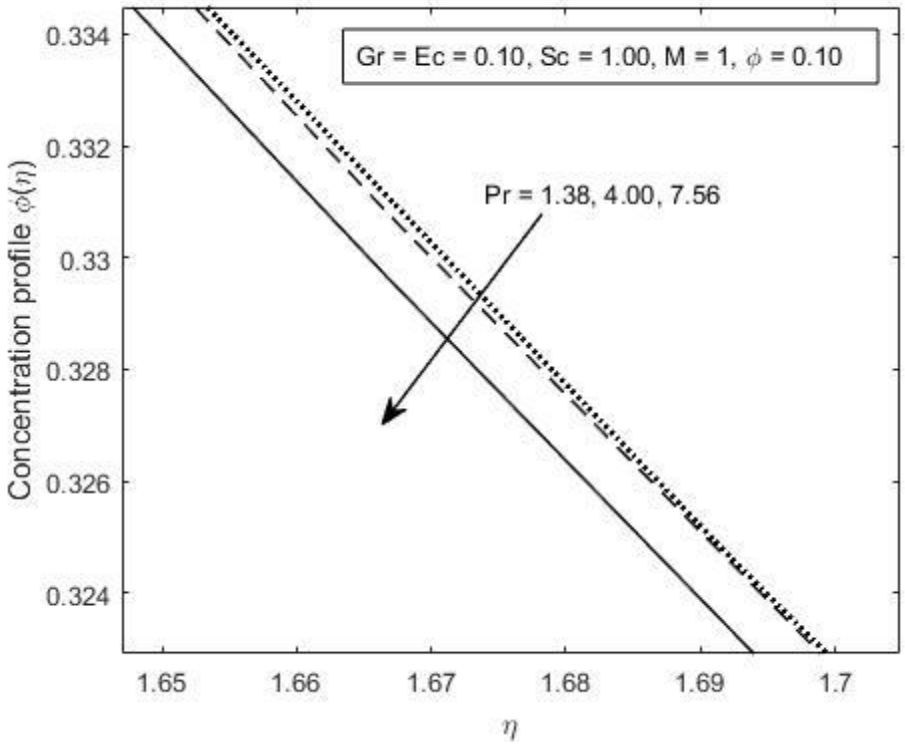

Figure 5.22: Concentration Profile for increasing Prandtl number

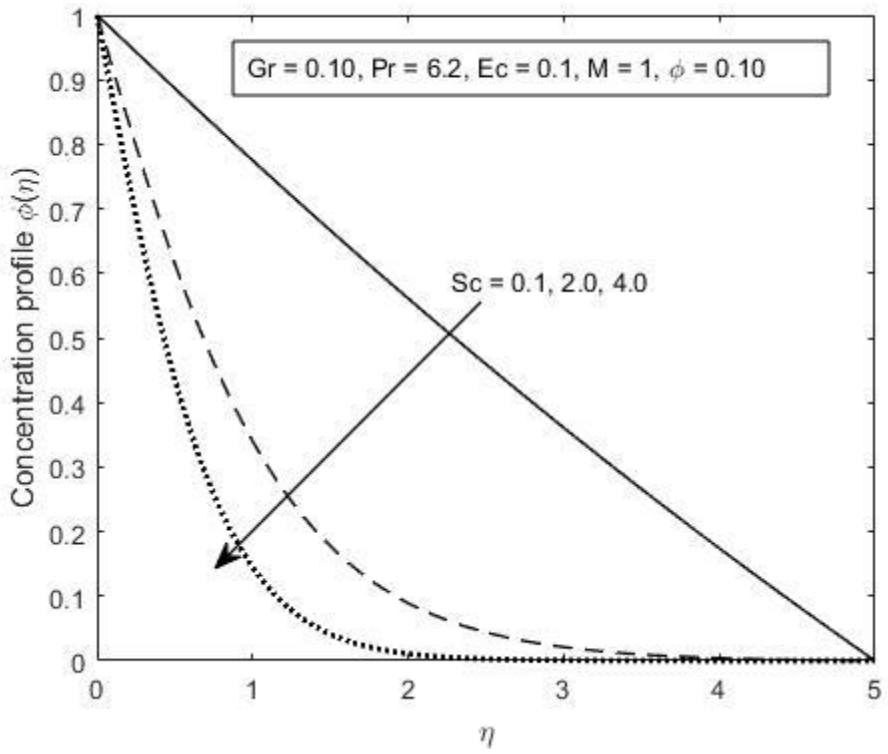

Figure 5.23: Concentration Profile for increasing Schmidt number

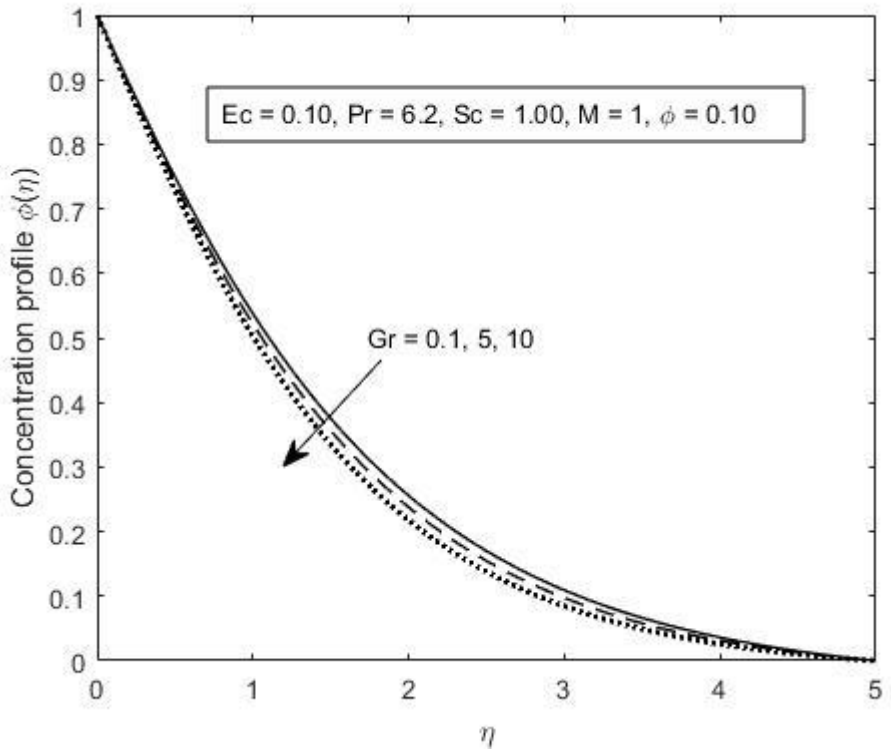

Figure 5.24: Concentration Profile for increasing Grashof number

5.1.4: Effects of variation of parameters on Skin friction, Nusselt number and Sherwood number on the two nanofluids.

The tables below shows values of Skin friction coefficient (cf), Nusselt number (Nu) and Sherwood number (Sh) when varying the Grashof number and the Eckert number while considering the two nanofluids.

5.1.4.1: Effects of varying the Grashof number on skin friction, Nusselt number and Sherwood number

Table 2 shows the effects of increasing the buoyancy forces leads to an increase in the skin friction and the Nusselt number but a decrease of the Sherwood number. The Al_2O_3-Ethylene Glycol nanofluid is showing a faster growth in the skin friction as compared to the Cu-Ethylene Glycol nanofluid. The Nusselt number is increasing at the same rate for both nanofluids while the Sherwood number is increasing at the same rate for both nanofluids too.

Table 2: Effects of varying Grashof number on skin friction, Nusselt number and Sherwood number

Gr	Ec	Sc	Pr	phi	cpnp	Nanoparticle	Cf	Nu	Sh
0.1	0.1	1	6.2	0.1	385	Cu	-1.41038	0.08757	-0.51928
0.1	0.1	1	6.2	0.1	765	Al2O3	-1.41037	0.08755	-0.51929
0.2	0.1	1	6.2	0.1	385	Cu	-1.40653	0.08758	-0.51968
0.2	0.1	1	6.2	0.1	765	Al2O3	-1.4065	0.08756	-0.51968
0.4	0.1	1	6.2	0.1	385	Cu	-1.39881	0.08759	-0.52047
0.4	0.1	1	6.2	0.1	765	Al2O3	-1.39876	0.08757	-0.52048
0.6	0.1	1	6.2	0.1	385	Cu	-1.39109	0.0876	-0.52127
0.6	0.1	1	6.2	0.1	765	Al2O3	-1.39101	0.08759	-0.52128
0.8	0.1	1	6.2	0.1	385	Cu	-1.38336	0.08762	-0.52207
0.8	0.1	1	6.2	0.1	765	Al2O3	-1.38325	0.0876	-0.52209
1	0.1	1	6.2	0.1	385	Cu	-1.37563	0.08763	-0.52287
1	0.1	1	6.2	0.1	765	Al2O3	-1.37549	0.08761	-0.52289

5.1.4.2: Effects of varying Eckert number on skin friction coefficient, Nusselt number and Sherwood number.

Table 3 below shows that an increase in the Eckert number leads to an increase in skin friction and a decrease in both the Nusselt number and the Sherwood number. The skin friction is seen to increase gradually for both nanofluids. The rate of heat transfer is seen to decrease rapidly when the Eckert number is increased.

Table 3: Effects of varying the Eckert number to skin friction, Nusselt number and the Sherwood number

Gr	Ec	Sc	Pr	phi	cpnp	Nanoparticle	Cf	Nu	Sh
0.1	0.1	1	6.2	0.1	385	Cu	-1.41038	0.08757	-0.51928
0.1	0.1	1	6.2	0.1	765	Al2O3	-1.41037	0.08755	-0.51929
0.1	0.2	1	6.2	0.1	385	Cu	-1.40685	0.0772	-0.51966
0.1	0.2	1	6.2	0.1	765	Al2O3	-1.40683	0.07718	-0.51967
0.1	0.4	1	6.2	0.1	385	Cu	-1.39978	0.0565	-0.52042
0.1	0.4	1	6.2	0.1	765	Al2O3	-1.39974	0.05649	-0.52043
0.1	0.6	1	6.2	0.1	385	Cu	-1.3927	0.03585	-0.52118
0.1	0.6	1	6.2	0.1	765	Al2O3	-1.39265	0.03585	-0.5212
0.1	0.8	1	6.2	0.1	385	Cu	-1.38562	0.01526	-0.52195
0.1	0.8	1	6.2	0.1	765	Al2O3	-1.38555	0.01526	-0.52196
0.1	1	1	6.2	0.1	385	Cu	-1.37853	-0.528	-0.52271
0.1	1	1	6.2	0.1	765	Al2O3	-1.37844	-0.528	-0.52274

5.1.4.3: Effects of increasing both the Grashof number and Eckert number on the skin friction coefficient, Nusselt number and Sherwood number for the two nanofluids

Increasing both the Grashof number and the Eckert number leads to a faster growth of the skin friction while the rate of heat transfer and mass transfer decreased at a faster rate as compared to when the parameters were varied independently. Al_2O_3-Ethylene Glycol based nanofluids showed a faster increase of the skin friction, while the Nusselt number and the Sherwood number varied at the same rate for both nanofluids.

Table 4: effects of varying both the Eckert number and the Grashof number on skin friction, Nusselt number and the Sherwood number

Gr	Ec	Sc	Pr	phi	cpnp	Nanoparticle	Cf	Nu	Sh
0.1	0.1	1	6.2	0.1	385	Cu	-1.41038	0.08757	-0.51928
0.1	0.1	1	6.2	0.1	765	Al2O3	-1.41037	0.08755	-0.51929
0.2	0.2	1	6.2	0.1	385	Cu	-1.39946	0.07723	-0.52044
0.2	0.2	1	6.2	0.1	765	Al2O3	-1.39941	0.07721	-0.52045
0.4	0.4	1	6.2	0.1	385	Cu	-1.35626	0.05681	-0.52509
0.4	0.4	1	6.2	0.1	765	Al2O3	-1.35611	0.0568	-0.52512
0.6	0.6	1	6.2	0.1	385	Cu	-1.28408	0.03694	-0.53306
0.6	0.6	1	6.2	0.1	765	Al2O3	-1.28376	0.03693	-0.53314
0.8	0.8	1	6.2	0.1	385	Cu	-1.18122	0.01768	-0.54485
0.8	0.8	1	6.2	0.1	765	Al2O3	-1.18067	0.01769	-0.54498
1	1	1	6.2	0.1	385	Cu	-1.04321	-0.00121	-0.5614
1	1	1	6.2	0.1	765	Al2O3	-1.04236	-0.0012	-0.56161

5.2: Conclusion

The effects of viscous dissipation and the magnetic field on the boundary layer of Ethylene-Glycol based nanofluids containing Copper and Alumina was studied theoretically while considering the thermophysical properties of the base fluid and the nanoparticles. The flow was considered to be past a heated vertical plate. The governing nonlinear partial differential equations were transformed into ordinary differential equations using a set of similarity variables. These equations were then solved numerically using the Runge-Kutta fourth-order method coupled with the shooting technique. The effects of the dimensionless parameters on

the velocity, temperature and concentration profile are analysed graphically while the effects of these parameters on skin friction, Nusselt number and Sherwood number are tabulated. Based on the above analysis, the following conclusions can be made:

- Velocity profiles increases with an increase in Eckert number and Grashof number but decreases with an increase in Magnetic field parameter. Variations of the Schmidt number, Prandtl number and the local Biot number have no effects to the momentum boundary layer.
- Temperature profiles increases with an increase in the Eckert number, Magnetic field parameter, Grashof number and the local Biot number while decreases with increase in the Prandtl number. Schmidt number has no effects in the thermal boundary layer.
- Concentration profiles increases with an increase in Magnetic field parameter but decreases with an increase in Eckert number, Schmidt number and the Grashof number. The local Biot number and the Prandtl number had no effect to the concentration boundary layer.
- Variation of Grashof number led to an increase in both the skin friction and the Nusselt number while a decrease in the Sherwood number. Variation of the Eckert number led to an increase of the skin friction but a decrease of both the Nusselt number and the Sherwood number.
- When both the Grashof number and the Eckert number were varied with equal values, an increase in the skin friction and a decrease in the Nusselt number and the Sherwood number were noted. This showed that the viscous forces were more dominant over the buoyancy forces.
- Al_2O_3-Ethylene glycol-based nanofluid had the highest skin friction while Cu-Ethylene glycol-based nanofluid had higher heat and mass transfer rates.

- From an engineering point of view, Cu-EG would make the best coolant due to its higher rate of heat transfer caused by a higher mass flow rate and that it causes less tear and wear on the plate surface due to minimal skin friction.
- Enhancement of metal nanoparticles in base fluids produces a better fluid as compared to the use of metal oxides nanoparticles.

5.3: Recommendations

Further research can be carried out by considering the presence of thermal radiation in an unsteady flow. A more complex geometric structure can also be considered.

REFERENCES

Amami, B., Dhahri, H., & Mhimid, A. (2014). Viscous dissipation effects on heat transfer, energy storage, and entropy generation for fluid flow in a porous channel submitted to a uniform magnetic field. *Journal of Porous Media*, *17*(10).

Basant k. Jha and Michael O. Oni. (2018). Mixed convection flow in a vertical channelwith temperature dependent viscosity and flow reversal: an exact solution. *International journalof heat and technology 36(2):607-613.*

Bergman, T. L., Incropera, F. P., DeWitt, D. P., & Lavine, A. S. (2011). *Fundamentals of heat and mass transfer*. John Wiley & Sons.

Choi, S. U., & Eastman, J. A. (1995). *Enhancing thermal conductivity of fluids with nanoparticles* (No. ANL/MSD/CP-84938; CONF-951135-29). Argonne National Lab., IL (United States).

Chrisholm, H. (Ed.). (1911). *The Encyclopædia britannica: a dictionary of arts, sciences, literature and general information* (Vol. 29). At the University press.

Desale, S., & Pradhan, V. H. (2015). Numerical solution of boundary layer flow equation with viscous dissipation effect along a flat plate with variable temperature. *Procedia Engineering*, *127*, 846-853.

Evans, W., Fish, J., & Keblinski, P. (2006). Role of Brownian motion hydrodynamics on nanofluid thermal conductivity. *Applied Physics Letters*, *88*(9), 093116.

https://sites.google.com/site/iranmhd/what-is-mhd

Jha, B. K., & Oni, M. O. (2018). Mixed convection flow in a vertical channel with temperature dependent viscosity and flow reversal: An exact solution. *Journal homepage: http://iieta. org/Journals/IJHT*, *36*(2), 607-613.

Khorasanizadeh, H., Fakhari, M. M., & Ghaffari, S. P. (2014). Investigation of Heat Transfer Enhancement or Deterioration of Variable Properties Al2O3-EG-water Nanofluid in Buoyancy Driven Convection. *Transp Phenom Nano Micro Scales*, *2*(1), 48-64.

Lakshmi, K. B., Raju, G. S. S., Kishore, P. M., & Rao, N. P. (2013). The Study of Heat Generation and Viscous Dissipation on MHD Heat and Mass Diffusion Flow Past A Surface. *IOSR Journal of Applied Physics*, *5*, 17-28.

Makinde, O. D. and Mutuku, W. N. (2014). Hydromagnetic thermal boundary layer of nanofluids over a convectively heated flat plate with viscous dissipation and ohmic heating. *UPB Sci Bull Ser A*, *76*(2), 181-192.

Makinde, O. D., & Olanrewaju, P. O. (2010). Buoyancy effects on thermal boundary layer over a vertical plate with a convective surface boundary condition. *Journal of Fluids Engineering*, *132*(4), 044502.

Mutuku, W. N. (2016). Ethylene glycol (EG)-based nanofluids as a coolant for automotive radiator. *Asia Pacific Journal on Computational Engineering*, *3*(1), 1.

Mutuku-Njane, W. N. (2014). *Analysis of hydromagnetic boundary layer flow and heat transfer of nanofluids* (Doctoral dissertation, Cape Peninsula University of Technology).

Nasrin, R., Alim, M. A., & Chamkha, A. J. (2012). Prandtl number variation on transient forced convection flow in a fluid valve using nanofluid. *International Journal of Engineering, Science and Technology*, *4*(2), 1-16.

Raza, J., Rohni, A., & Omar, Z. (2016). Numerical investigation of copper-water (Cu-water) nanofluid with different shapes of nanoparticles in a channel with stretching wall: slip effects. *Mathematical and Computational Applications*, *21*(4), 43.

Rossow, V. J. (1958). On flow of electrically conducting fluids over a flat plate in the presence of a transverse magnetic field.

Sekrani, G., & Poncet, S. (2018). Ethylene-and Propylene-Glycol Based Nanofluids: A Litterature Review on Their Thermophysical Properties and Thermal Performances. *Applied Sciences*, *8*(11), 2311.

Seyyedi, S. M., Dogonchi, A. S., Hashemi-Tilehnoee, M., & Ganji, D. D. (2019). Improved velocity and temperature profiles for integral solution in the laminar boundary layer flow on a semi-infinite flat plate. *Heat Transfer—Asian Research*, *48*(1), 182-215.

Sivaiah, S. (2013). MHD flow of a rotating fluid past a vertical porous flat plate in the presence of chemical reaction and radiation. *Journal of Engineering Physics and Thermophysics*, *86*(6), 1328-1336.

Uddin, M. J., Khan, W. A., & Ismail, A. I. (2012). MHD free convective boundary layer flow of a nanofluid past a flat vertical plate with Newtonian heating boundary condition. *PLoS One*, *7*(11), e49499.

Vajravelu, K., & Prasad, K. V. (2012). Heat transfer phenomena in a moving nanofluid over a horizontal surface. *Journal of Mechanics*, *28*(3), 579-588.

William Evans,Jacob Fish and Pawel Keblinski.(2006).Role of Brownian Motion hydrodynamics on nanofluid thermal conductivity. *APPLIED PHYSICS LETTERS,88(093116)*

Zhao, G. P., Jian, Y. J., & Li, F. Q. (2017). Electromagnetohydrodynamic Flow and Heat Transfer of Nanofluid in a Parallel Plate Microchannel. *Journal of* Mechanics, *33*(1), 115-124.